Stereochemical Alterations of ^{2}E Chromium(III) Excited-State Behavior in Dicyanotetraazacyclotetradecane Complexes. Ground-State X-ray Crystal Structures, Photophysical Behavior, and Molecular Mechanics Simulations of Stereochemical Effects[1]

Ronald B. Lessard, Mary Jane Heeg, Tione Buranda, Marc W. Perkovic, Carolyn L. Schwarz, Yang Rudong, and John F. Endicott*

Department of Chemistry, Wayne State University, Detroit, Michigan 48202

Received July 3, 1991

Comparisons have been made of the stereochemistries of several $Cr^{III}(N_4)X_2$ complexes and their photophysical behaviors, where N_4 is a macrocyclic tetraamine and X is CN^- or NH_3. The trans complexes tend to have (^{2}E)-Cr(III) excited-state lifetimes which are about 2 orders of magnitude longer than those of their cis analogs under ambient conditions. This trans:cis lifetime ratio increased about 10-fold when the coordinated amines were per-deuterated, and some of the cyano–tetraamine-d_4 complexes had 2–4-ms lifetimes in D_2O solutions at 25 °C. Stereochemical perturbations have been introduced by means of complexes containing methyl group substituents (C-CH_3), in the tetraamine ligand which assume positions near the Cr–X coordination sites. Ground-state geometries of the methylated complexes have been determined by X-ray crystallography. The influence of these stereochemical perturbations on potential associative or dissociative relaxation coordinates has been modeled using MM2 approaches. The results of the MM2 calculations have been compared to the experimental results for (^{2}E)Cr(III) relaxation and found to support the hypothesis that the more facile relaxation of the *cis*-$Cr^{III}(N_4)X_2$ complexes is largely a stereochemical effect. The effects of these simple stereochemical perturbations on (^{2}E)Cr(III) lifetimes suggest that the predominant relaxation pathway could have either associative or dissociative components and that the nature of the predominant components changed from dissociative to associative when X was changed from NH_3 to CN^- in *trans*-$Cr(N_4)X_2$ complexes. Overall, simple, limiting back-intersystem-crossing or doublet-state reaction models do not account for the (^{2}E)Cr(III) excited-state relaxation behavior found for these am(m)ine or cyanoam(m)ine complexes. Rather it is proposed that the thermally activated decay is the result of nuclear distortions which relax the electronic constraints on excited-state decay. [*trans*-Cr(5,12-*meso*-5,7,7,12,14,14-hexamethyl-1,4,8,11-tetraazacyclotetradecane)$(OH_2)OH](ClO_4)_2 \cdot H_2O$, $CrN_4C_{16}H_{41}O_{11}Cl_2$, crystallized in the triclinic space group $P\bar{1}$ with $Z = 2$, $a = 10.217$ (1) Å, $b = 11.071$ (1) Å, $c = 12.824$ (1) Å, $\alpha = 99.49$ (1)°, $\beta = 95.73$ (1)°, $\gamma = 112.86$ (1)°. The structure refined to $R = 0.048$ and $R_w = 0.045$ using 4472 observed reflections. [*cis*-Cr(5,12-*rac*-5,7,7,12,14,14-hexamethyl-1,4,8,11-tetraazacyclotetradecane)$(CN)_2$]Cl, $CrC_{18}H_{36}N_6Cl$, crystallized in the orthorhombic space group *Fd2d* (nonstandard setting of *Fdd*2, No. 43) with $Z = 8$, $a = 9.362$ (1) Å, $b = 12.866$ (2) Å, and $c = 34.742$ (7) Å. The structure refined to $R = 0.033$ and $R_w = 0.030$ using 1922 observed reflections.

Introduction

An understanding of the reactive and nonreactive relaxation mechanisms of transition metal excited states is a necessary prerequisite for their rational utilization as mediators of chemical reactions, energy conversion, etc. As in any mechanistic analysis, such an understanding of excited-state decay dynamics must relate information about the accompanying changes in molecular structure and energy to the basic kinetic behavior. One should then be able to use a successful mechanistic model to design molecules in which molecular structure changes can be inhibited or promoted and/or the energies between the important states altered. A potentially powerful means of manipulating excited-state lifetimes would be through stereochemical variations of the coordinated ligands. The modification of transition metal excited-state lifetimes and reactivities by means of stereochemical perturbations would raise the possibility of the design of electronically excited species to function in specific chemical or physical roles. Such stereochemical alterations of the decay patterns of electronic excited states should be most important for ambient conditions, since the role of stereochemistry in altering reaction patterns is usually to promote or repress thermally activated nuclear motions. Ambient excited-state lifetimes, τ, generally decrease as the temperature increases:[2,3]

$$\tau^{-1} = k = k_{lim} + k(T) \quad (1)$$

where k_{lim} is the nearly temperature- and medium-independent decay rate constant observed at low temperatures and $k(T)$ describes the temperature- (and medium-) dependent decay behavior. This one expects that stereochemical perturbations can make major contributions to excited-state lifetimes only to the extent that $k(T)$ reflects the energetics required for nuclear reorganization along the relaxation pathway. If $k(T)$ is largely determined by the thermal population of an upper excited state, as in back intersystem crossing (BISC; process a in Figure 1), then one expects purely stereochemical effects to be relatively insignificant. Thus, stereochemical perturbations often have very specific mechanistic implications, and this has been of interest to us for some time.[2,4-6] This interest has been in part stimulated by the demonstration by Kane-Maguire and co-workers[7] that

(1) Partial support of this research by the Division of Chemical Sciences, Office of Basic Energy Sciences, Office of Energy Research, U.S. Department of Energy, is gratefully acknowledged.

(2) Endicott, J. F.; Ramasami, T.; Tamilarasan, R.; Lessard, R. B.; Ryu, C. K.; Brubaker, G. R. *Coord. Chem. Rev.* **1987**, *77*, 1.
(3) Forster, L. S. *Chem. Rev.* **1990**, *90*, 331.
(4) (a) Endicott, J. F.; Lessard, R. B.; Lei, Y.; Ryu, C. K.; Tamilarasan, R. *Excited States and Reactive Intermedites*; Lever, A. B. P., Ed.; ACS Symposium Series 307; American Chemical Society: Washington, DC, 1986; p 85. (b) Endicott, J. F.; Ryu, C. K.; Lessard, R. B.; Hoggard, P. E. *In Photochemistry and Photophysics of Coordination Compounds*; Vogler, A., Yersin, H., Eds.; Springer-Verlag: Berlin, 1987; p 40. (c) Endicott, J. F.; Lessard, R. B.; Lynch, D.; Perkovic, M. W.; Ryu, C. K. *Coord. Chem. Rev.* **1990**, *97*, 65.
(5) Lessard, R. B. Ph.D. Dissertation, Wayne State University, 1988.

0020-1669/92/1331-3091$03.00/0

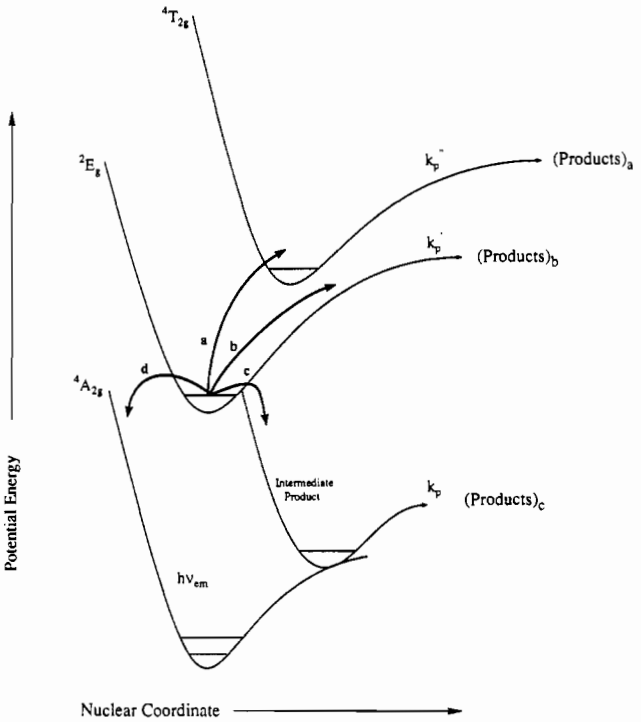

Figure 1. Qualitative illustration of different classes of (^{2}E)Cr(III) relaxation pathways: (a) back intersystem crossing; (b) direct chemical reaction to form electronically correlated products; (c) relaxation to form an intermediate species with the ground-state electronic configuration but a nonequilibrium molecular geometry; (d) direct relaxation to the undistorted ground state. Components of pathway d, which is the only available relaxation route at low temperatures, are radiative (k_r) and nonradiative ($k°_{nr}$) so that $k_{lim} = [\tau(77\ K)]^{-1} = k_r + k°_{nr}$. All other relaxation pathways are expected to be thermally activated, so that $[\tau(T)]^{-1} = k_{lim} + k(T)$.

trans-(^{2}E)Cr([14]aneN$_4$)(NH$_3$)$_2^{3+}$ [8] is nearly photoinert[7] and that its ambient solution lifetime is only weakly temperature dependent,[9] in contrast to the behavior of the cis analog.[7,9] However, this contrast in the photophysics of these *cis*- and *trans*-diammine complexes might be attributable to some factor other than stereochemistry; e.g., back intersystem crossing to a low-energy quartet excited state might be more important in the cis than in the trans complex.[10,11] However, there are reasons to believe that BISC is relatively insignificant for hexam(m)ine complexes.[12-14] Furthermore, even if the contrasts in thermally activated relaxation rates of cis and trans (^{2}E)Cr(III) complex excited states were stereochemical, the net relaxation process might be a composite of a number of pathways. Some possible examples are (i) association with a solvent molecule, (ii) dissociation of a monodentate ligand, and (iii) folding of the macrocyclic ligand to achieve the coordination environment of some ground-state intermediate species.

Our systematic studies of these problems have involved[2,4-6,12] (a) X-ray structural determinations of ground-state geometries, (b) spectroscopic investigations of any significant excited-state distortions, (c) spectroscopic determinations of excited-state energies, and (d) molecular mechanics simulations of the effects of ligand stereochemistry on potential relaxation coordinates, as well as (e) a range of studies of excited-state relaxation dynamics. The present work reports our studies of several Cr(N$_4$)(CN)$_2^+$ and Cr(N$_4$)(NH$_3$)$_2^{3+}$ complexes (where N$_4$ is a tetraazamacrocyclic ligand). While this work was in progress, Waltz and co-workers[10a] published some very interesting evidence that a chemical intermediate is formed in the decay of *cis*-(^{2}E)Cr([14]aneN$_4$)(NH$_3$)$_2^{3+}$ and that this intermediate seemed to be a 7-coordinate Cr([14]aneN$_4$)(NH$_3$)$_2$OH$_2^{3+}$ species, lending credibility to a relaxation pathway such as (i). In a very recent elaboration of this work, Friesen et al.[10b] report small positive volumes of activation for doublet decay of both the *cis*- and *trans*-(^{2}E)Cr([14]aneN$_4$)(NH$_3$)$_2^{3+}$ complexes and Arrhenius activation energies of $E_A = 9$ and 14 kcal mol^{-1}, respectively [for $k(T) = A\exp(-E_A/RT)$]. These authors attribute this contrast in excited-state decay behavior to a BISC mechanism, with the intermediate being formed from an excited quartet state. Kirk and Heyd have made a closely related argument supporting this view.[11] Surprisingly, the Arrhenius pre-exponential factors were found to be vastly different for the cis and trans complexes, $A = 1 \times 10^{12}$ and 5×10^4 s^{-1}, respectively,[10b] suggesting the contributions of different decay channels.[15] In contrast, very recent studies from this laboratory have indicated that certain nuclear motions of the complex ligands can dominate thermally activated (^{2}E)Cr(III) relaxation.[4c,6] With a view to elucidating the influence of macrocyclic ligand stereochemistry on the photophysics of *cis*- and *trans*-Cr^{III}(N$_4$)X$_2$ complexes (where N$_4$ is a tetraazamacrocyclic ligand), we decided to investigate the behavior of a *cis*-Cr(N$_4$)(CN)$_2^+$ complex in order to provide a stereochemical contrast to the *trans*-Cr([14]aneN$_4$)(CN)$_2^+$, complex which has been shown to have a nearly temperature-independent ^{2}E excited-state lifetime.[16] Our attempts to prepare *cis*-Cr([14]aneN$_4$)(CN)$_2^+$ failed, apparently due to base-catalyzed cis–trans isomerizations and the greater stability of the *trans*-dicyano complex. As a consequence, we have used the *rac*-(5,12)-Me$_6$[14]aneN$_4$[8] ligand (see Figure 2), which has a stereochemical propensity for formation of cis complexes.[17,18] The use of the methyl-substituted [14]aneN$_4$ ligand has necessitated the synthesis and photophysical characterization of several related macrocyclic ligand complexes. In the course of this study, we have determined the X-ray crystal structures of [*cis*-Cr(*rac*-(5,12)-Me$_6$[14]aneN$_4$)(CN)$_2$]Cl and [*trans*-Cr(*ms*-(5,12)-Me$_6$[14]aneN$_4$)(OH)(OH$_2$)](ClO$_4$)$_2$, and we have used molecular mechanics methods to explore several ways in which stereochemical effects might influence excited-state lifetimes. Our observations on these systems substantially confirm that stereochemical factors can play a very important and sometimes dominant role in dictating transition metal excited-state behavior.[19]

(6) (a) Perkovic, M. W.; Endicott, J. F. *J. Phys. Chem.* **1990**, *94*, 1217. (b) Perkovic, M. W.; Endicott, J. F. *Inorg. Chem.* **1991**, *30*, 3140.
(7) Kane-Maguire, N. A. P.; Wallace, K. C.; Miller, D. B. *Inorg. Chem.* **1985**, *24*, 597.
(8) Abbreviations: [14]aneN$_4$ = cyclam = 1,4,8,11-tetraazacyclotetradecane; [15]aneN$_4$ = 1,4,8,12-tetraazacyclopentadecane; *ms*-(5,12)-Me$_6$[14]aneN$_4$ = tet*a* = 5,12-*meso*-5,7,7,12,14,14-hexamethyl-1,4,8,11-tetraazacyclotetradecane; *rac*-(5,12)-Me$_6$[14]aneN$_4$ = tet*b* = 5,12-*rac*-5,7,7,12,14,14-hexamethyl-1,4,8,11-tetraazacyclotetradecane; sen = 4,4',4''-ethylidynetris(3-azabutan-1-amine); [9]aneN$_3$ = 1,4,7-triazacyclononane; TAP[9]aneN$_3$ = 1,4,7-tris(aminopropyl)-1,4,7-triazacyclononane; TAE[9]aneN$_3$ = 1,4,7-tris(2-aminoethyl)-1,4,7-triazacyclononane; (([9]aneN$_3$)CH$_2$–)$_2$ = 1,2-bis(1,4,7-triaza-1-cyclononyl)ethane.
(9) Fucaloro, A. F.; Forster, L. S. *Inorg. Chim. Acta* **1987**, *132*, 253.
(10) (a) Waltz, W. L.; Lee, S. H.; Friesen, D. A.; Lilie, J. *Inorg. Chem.* **1988**, *27*, 1132. (b) Friesen, D. A.; Lee, S. H.; Lilie, J.; Waltz, W. L.; Vincze, L. *Inorg. Chem.* **1991**, *30*, 1975.
(11) Kirk, A. D.; Heyd, D. *Inorg. Chem.* **1991**, *30*, 2453.
(12) Lessard, R. B.; Endicott, J. F.; Perkovic, M. W.; Ochrymowycz, L. A. *Inorg. Chem.* **1989**, *28*, 2474.
(13) Forster, L. S.; Murrow, D.; Fucaloro, A. F. *Inorg. Chem.* **1990**, *29*, 3706.
(14) It is important to bear in mind our earlier observation that when weak field ligand (X) are employed in the Cr(N$_4$)X$_2$ complexes, so that the energy differences between the doublet and quartet excited states are small, the cis and trans complexes are found to have comparable photophysical behaviors.[12]
(15) Note that a pre-exponential factor of $A = 10^{12}$–10^{13} s^{-1} is expected for an electronically allowed surface crossing, so that one might infer an electronically allowed relaxation pathway for the cis complex and an electronically forbidden pathway for the trans.
(16) Kane-Maguire, N. A. P.; Crippen, W. S.; Miller, P. K. *Inorg. Chem.* **1983**, *22*, 696.
(17) (a) Curtis, N. F. In *Coordination Chemistry of Macrocyclic Compounds*; Melson, G. A., Ed.; Plenum: New York, 1979; Chapter 4. (b) Whimp, P. O.; Bailey, M. F.; Curtis, N. F. *J. Chem. Soc. A* **1970**, 1956.
(18) Kane-Maguire, N. A. P.; Endicott, J. F.; Rillema, D. P. *Inorg. Chim. Acta* **1972**, *6*, 443.
(19) Preliminary reports of some of our observations have appeared in ref 4.

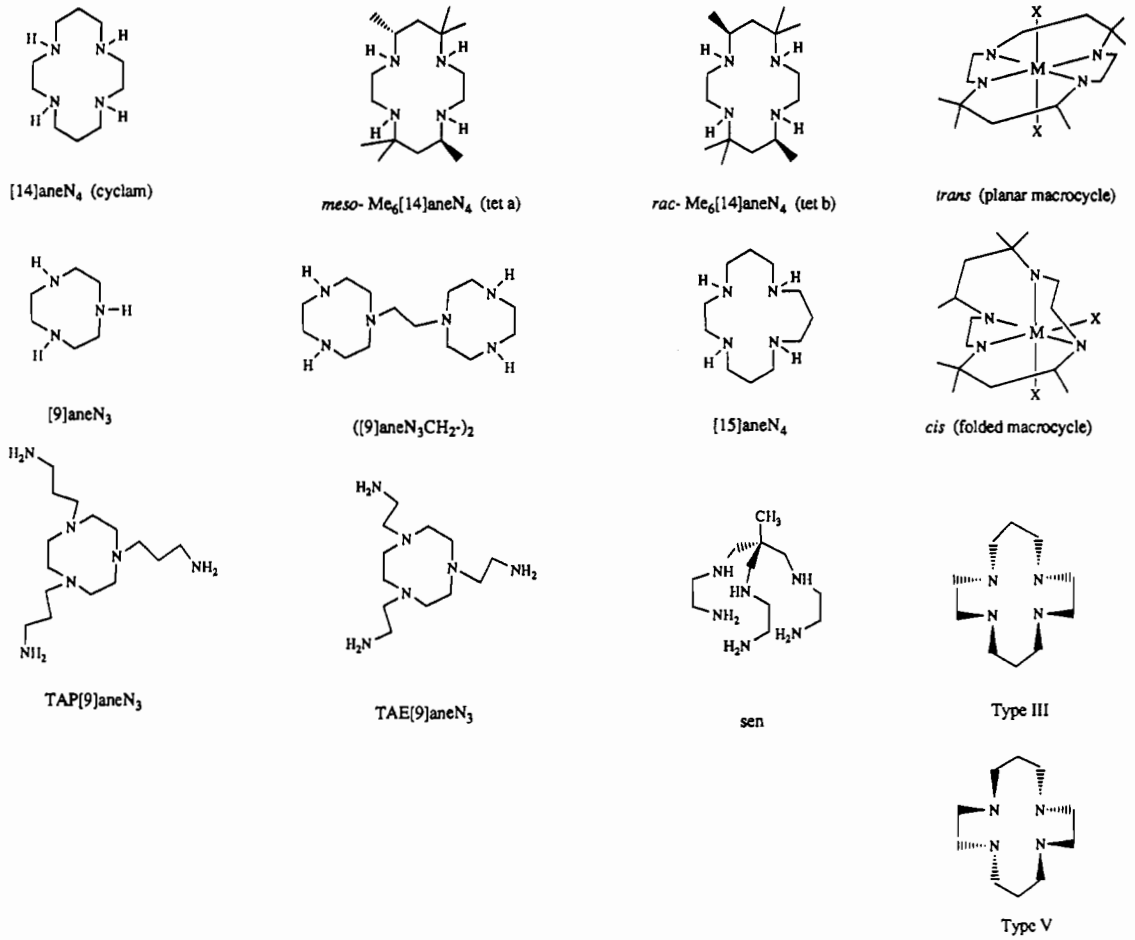

Figure 2. Skeletal structures of macrocyclic ligands and possible isomers of complexes with the [14]aneN$_4$ ligands.

Experimental Section

A. Preparation of Complexes. Literature syntheses were used for the complexes[8] *trans*-Cr^{III}([14]aneN$_4$)X$_2$ (X = CN$^-$ [16] and NH$_3$[7,18]), *cis*-Cr([14]aneN$_4$)(NH$_3$)$_2^{3+}$,[7,18] *trans*-Rh([14]aneN$_4$)(CN)$_2^+$,[20] [*cis*(Cr(*rac*-(5,12)-Me$_6$[14]aneN$_4$)(OH$_2$)$_2$](ClO$_4$)$_3$,[21] *trans*-Cr(*ms*-(5,12)-Me$_6$[14]-aneN$_4$)(NH$_3$)$_2$](ClO$_4$)$_3$,[20] and [*trans*-Cr([15]aneN$_4$)Cl$_2$]ClO$_4$.[12] The [15]aneN$_4$ ligand was purchased from Strem Chemical Co. The other macrocyclic ligands were synthesized as noted in the literature cited. Commercial HCF$_3$SO$_3$ was added to solid NaCO$_3$ to obtain NaCF$_3$SO$_3$. The dried solid was purified by recrystallization from methanol.

Caution! The perchlorate salts prepared in this study are potentially explosive and should be handled with very great care.

[*trans*-Cr(*ms*-(5,12)-Me$_6$[14]aneN$_4$)(OH)OH$_2$]ClO$_4$·H$_2$O. The material with this stoichiometry crystallized when a solution of [Cr(*ms*-(5,12)-Me$_6$[14]aneN$_4$)(OH$_2$)$_2$](ClO$_4$)$_3$ in 0.1 M aqueous NaOH was incompletely acidified.

[*trans*-Cr(*ms*-(5,12)-Me$_6$[14]aneN$_4$)(CN)$_2$]ClO$_4$. The [*trans*-Cr(*ms*-(5,12)-Me$_6$[14]aneN$_4$)Cl$_2$]ClO$_4$[21,22] salt (1.5 g) was dissolved in 20 mL of DMSO, and the solution was heated to 76 °C; then 0.8 g of finely ground NaCN was added to the hot solution. After a minute or so, the green solution began to turn red, and it eventually became brown-yellow. The temperature was maintained at 60 °C for approximately 2 h, or until a yellow solid began to form. The preparative mixture was cooled to room temperature and filtered, and the solid was washed with ethanol and ethyl ether. The crude product was dissolved in about 1.5 L of H$_2$O, and solid NaClO$_4$ was added to precipitate the complex. The yield was 1.0 g or 69%. Anal. Found (calcd for CrC$_{18}$H$_{36}$N$_6$ClO$_4$): C, 42.07 (41.98); H, 7.63 (7.63); N, 16.21 (16.32); Cr, 9.6 (9.2). This complex had absorption maxima at 337 ± 1 and 427 ● 1 nm (ϵ = 59 and 63 cm^{-1} M^{-1}, respectively, in water) which were solvent independent (in acetonitrile, DMSO, and water).

[*cis*-(Cr(*rac*-(5,12)-Me$_6$[14]aneN$_4$)(OH$_2$)$_2$](CF$_3$SO$_3$)$_3$. The [*cis*-Cr(*rac*-(5,12)-Me$_6$[14]aneN$_4$)Cl$_2$]Cl[21] complex (5 g) was dissolved in a solution of 2 g of NaOH in 50 mL of water. The blue solution was cooled to 0 °C, and 10 mL of concentrated HCF$_3$SO$_3$ was added slowly.[23] The resulting mixture was filtered and dried in vacuo. The yield was 6.3 g or 100%.

[*cis*-(Cr(*rac*-(5,12)-Me$_6$[14]aneN$_4$)(CN$_2$)$_2$]Cl. The diaquo complex (1.0 g), prepared as above, was added to 20 mL of DMSO, and the mixture was heated to 170 °C for 20 min. The temperature was reduced to 80 °C, and 0.8 g of NaCN was added. The solution was kept at 80 °C for 10 min, during which time an orange solid began to form. The mixture was cooled to room temperature and filtered. The orange solid was washed with ethanol and ethyl ether and dried in vacuo. The yield was 0.4 g or 60%. Anal. Found (calcd for CrC$_{18}$H$_{36}$N$_6$Cl): C, 41.53 (41.07); H, 6.94 (6.89); N, 15.02 (15.13); Cr, 9.2 (9.3). This complex had three d–d absorption maxima: a high-energy band at 347 ± 1 nm independent of solvent and a pair of peaks centered at about 460 nm. The resolutions of the low-energy d–d transitions were notably solvent dependent: the high-energy component was dominant in water with an apparent maximum at 447 nm (ϵ = 112 cm^{-1} M^{-1}) and a shoulder at about 462 nm (ϵ = 110 cm^{-1} M^{-1}), while the low-energy component was a more dominant feature in acetone, acetonitrile, DMSO, and methanol (apparent maxima at 432 and 489 nm, 437 and 489 nm, 440 and 489 nm, and 437 and 481 nm, respectively; intensity ratios were about 0.97:1 in the first three solvents and about 1.0:1.0 in methanol).

[*trans*-Cr([15]aneN$_4$)Cl$_2$]ClO$_4$. A solution of 1.0 g of [15]aneN$_4$ and 2.0 g of Cr(THF)$_3$Cl$_3$[24] (THF = tetrahydrofuran) in 20 mL of dry DMF was refluxed for 10 min. A green solid formed on the bottom of the flask as it cooled and was removed by filtration. A second crop of green solid,

(20) Kane-Maguire, N. A. P.; Wallace, K. C.; Trzaperk, T. S. *Inorg. Chim. Acta* **1983**, *76*, L179.
(21) (a) House, D. A.; Hay, R. W.; Akbar, A. M. *Inorg. Chim. Acta* **1983**, *72*, 239. (b) Barefield, E. K.; Wagner, F.; Herlinger, A. W.; Dahl, A. R. *Inorg. Synth.* **1976**, *16*, 220.
(22) Hay, R. W.; Lawrence, A. *J. Chem. Soc., Perkin Trans. 1* **1975**, 591.
(23) A related synthesis has been reported using HBr rather than HCF$_3$SO$_3$: Eriksen, J.; Mønsted, O. *Acta Chem. Scand.* **1983**, *37*, 585.
(24) This complex was synthesized by Professor G. R. Brubaker. It is also available from Aldrich Chemical Corp.

obtained when the filtrate was reduced in volume by 50%, was combined with the first, and the total was washed with cold acetone and ether. The resulting green solid was dissolved in the minimum amount of water and precipitated with concentrated $HClO_4$. The solid was collected by filtration and washed with acetone and ether. The yield was 0.26 g or 89%. Anal. Found (calcd for $CrC_{11}H_{26}N_4Cl_3O_4$): C, 30.13 (30.25); H, 6.06 (6.00); N, 12.71 (12.83).

[*trans*-Cr([15]aneN$_4$)(CN)$_2$]ClO$_4$. A mixture of 0.14 g of [*trans*-Cr([15]aneN$_4$)Cl$_2$]ClO$_4$, 0.09 g of NaCN, 1.1 mL of DMSO was heated to 62 °C for 1 h. The yellowish brown solid that formed by filtration after the solution cooled and washed with acetone and ether. The yield was 0.11 g or 82%. This material was dissolved in the minimum amount of water and precipitated by the addition of $NaClO_4$. The final product was collected as bright yellow crystals. Anal. Found (calcd for $CrC_{13}H_{26}N_6O_4Cl\cdot NaClO_4$): C, 29.12 (28.90); H, 5.31 (4.85); N, 15.75 (15.56). The complex had absorption maxima at 348 and 452 nm.

[*cis*-Rh(*rac*-(5,12)-Me$_6$[14]aneN$_4$)Cl$_2$]Cl·3H$_2$O. A solution of 1.05 g of $RhCl_3\cdot 3H_2O$ in 40 mL of DMF was boiled for 5 h. This was combined with 15 mL of a DMF solution of *rac*-(5,12)-Me$_6$[14]aneN$_4$·H$_2$O (which had also been boiled to remove H_2O). The combined solution changed color from red to yellow, and a solid formed. The solid was collected after cooling and recrystallized from water. Anal. Found (calcd for $RhC_{16}H_{34}N_4Cl_3\cdot 3H_2O$): C, 35.39 (35.47); H, 6.95 (7.8); N, 9.81 (10.34).

[Rh(Me$_6$[14]aneN$_4$)(CN)$_2$]PF$_6$. Dicyano complexes were formed from the respective Rh(Me$_6$[14]aneN$_4$)Cl$_2^+$ salts (preceding) by adding NaCN to their DMF solutions. The resulting complexes were dissolved in water and reprecipitated as the PF_6^- salts. Anal. Found (calcd for the [*cis*-Rh(*rac*-(5,12)-Me$_6$[14]aneN$_4$)(CN)$_2$]PF$_6$·H$_2$O complex salt ($RhC_{18}H_{34}N_6PF_6H_2O$)): C, 36.15 (35.86); N, 13.56 (13.94); H, 6.22 (6.37).

Samples with Cr(N$_4$)(CN)$_2^+$ (N$_4$ = [14]aneN$_4$ or *rac*-(5,12)-Me$_6$[14]aneN$_4$) doped into a rhodium(III) complex salt were prepared by dissolving a weighed amount of the appropriate Rh(III) complex in water, adding 1–3 mol % of the [Cr(N$_4$)(CN)$_2$]ClO$_4$ salt to the solution, and adding $NaClO_4$ to precipitate the desired solid.

Amine deuteration was accomplished by successive recrystallizations from D_2O. The extent of deuteration was monitored by determining the intensity ratio of the N–H to the N–D stretching frequencies in the recrystallized solids.

B. Instrumental Techniques. The procedures used for determining excited-state emission spectra and decay rates have been described elsewhere.[12,25] The emission spectra were obtained using a Princeton Instruments IRY 512 diode array system (PI-DARS) with an ST-120 controller. The PI-DARS was wavelength-calibrated using the emission of a Phillips Ne resonance lamp. Corrections for detector distortions were based on diffuse white light from a tungsten source projected directly onto the detector. A power series correction curve was constructed on the basis of the average of the relative diode responses for (a) diffuse white light projected onto the detector (no monochromator) and (b) the zero-order reflection of the Jarrell-Ash monochromator targeted in turn on every 10th diode.

C. X-ray Structure Determinations. Table I contains a summary of the crystallographic experimental data. Additional parameters in common are given now in abbreviated form: Nicolet R3 diffractometer, graphite monochromator, Mo Kα (λ = 0.710 73 Å), 298 (2) °C, scan method $\theta/2\theta$, scan range 1.0° below Kα_1 to 1.0° above Kα_2, empirical absorption corrections via SHELXTL,[26] no correction for extinction, solution by Patterson methods, refinement in a full matrix in SHELX-76[27] on F's minimizing $\sum w(F_o-|F_c|)^2$, all non-hydrogen atoms anisotropic, neutral-atom scattering factors from ref 28.

For [*trans*-Cr(*ms*-(5,12)-Me$_6$[14]aneN$_4$)(OH)(OH$_2$)](ClO$_4$)$_2$, hydrogen atoms were placed in observed positions and refined. The maximum residual electron density in a final ΔF map represented 0.98 e/Å^3 in the perchlorate region.

For [*cis*-Cr(*rac*-(5,12)-Me$_6$[14]aneN$_4$)(CN)$_2$]Cl, hydrogen atoms were placed in observed positions and held variant with all U(H) tied to a single variable. The largest peak on a final ΔF map represented 0.6 e/Å^3.

Table I. Crystallographic Data for Cr^{III}(Me$_6$[14]aneN$_4$) Complexes

	[Cr(*ms*-(5,12)-Me$_6$[14]aneN$_4$)(OH$_2$)(OH)](ClO$_4$)$_2$·H$_2$O	[Cr(*rac*-(5,12)-Me$_6$[14]aneN$_4$)(CN)$_2$]Cl
formula	$CrC_{16}H_{41}N_4O_{11}Cl_2$	$CrC_{18}H_{36}N_6Cl$
mol wt	588.43	423.98
space group	$P\bar{1}$	*Fd2d* (nonstandard setting of *Fdd*2, No. 43)
a, Å	10.271 (1)	9.362 (1)
b, Å	11.071 (1)	12.866 (2)
c, Å	12.824 (1)	34.742 (7)
α, deg	99.49 (1)	
β, deg	95.73 (1)	
γ, deg	112.86 (1)	
V, Å^3	1296.7 (2)	4185 (1)
T, °C	25	25
λ, Å	0.710 73	0.710 73
Z	2	8
ρ_{calc}, g cm^{-3}	1.507	1.346
μ, cm^{-1}	6.9	7.1
R, R_w[a]	0.048, 0.045	0.033, 0.030

[a] $R = (\sum||\Delta F|)/(\sum|F|)$; $R_w = [(\sum w|\Delta F|^2)/(\sum wF_o^2)]^{1/2}$.

An inversion of polarity produced significantly higher R values: R = 0.042, R_w = 0.037 compared to R = 0.033, R_w = 0.030.

D. Molecular Mechanics Calculations. Several possible models for the contributions of the macrocyclic ligand to the excited-state relaxation dynamics were evaluated by means of a locally modified version[29] of the Allinger–Yuh MM2/MMP2 program.[30] The total energy of the complex with a given set of atomic coordinates was calculated on the basis of the sum of individual interactions (comp = compression; dip = dipole; tor = torsion; vdW = van der Waals):

$$E_{tot} = E_{comp} + E_{bend} + E_{vdW} + E_{dip} + E_{tor}$$

These interaction energies were defined as in the Allinger–Yuh program. The initial atomic coordinates were based on the X-ray structures of [*trans*-Cr(*ms*-(5,12)-Me$_6$[14]aneN$_4$)(OH)OH$_2$](ClO$_4$)$_2$ and [*cis*-Cr(*rac*-(5,12)-Me$_6$[14]aneN$_4$)(CN)$_2$]Cl. Interaction parameters for the C, H, and N atoms of the macrocyclic ligand were as defined in the program. Torsional parameters for motions around the metal were set equal to zero,[29,31] and other interaction constants involving the metal either were based on the values tabulated by Brubaker and Johnson[31] or were reported vibrational frequencies. Dipolar interactions not involving shared atoms were included in the calculations; metal–ligand dipole moments were based on differences in optical electronegativities.[32] The calculational strategy was based on evaluating the contributions of the macrocyclic ligand to the distortion coordinate. To accomplish this, the interaction parameters (except van der Waals interactions) of the leaving group X (or the entering group in associative pathways) were subtracted from the minimized energy to obtain the final "residual steric energy", E_s, for each metal–X distance. A table of typical interaction constants is included in the supplementary material.[33] More detailed descriptions of our procedures and their application to the evaluation of thermal substitution in ground-state species may be found elsewhere.[29]

E. Excited-State Quenching Studies. Excited-state lifetimes were determined using our standard procedures[12,25] in aqueous solutions of different concentrations of NaSCN or $Na_2S_2O_3$ at 25 °C. Ionic strengths were maintained constant at 1.0 with $NaCF_3SO_3$ when possible. Ionic strengths were variable when the total salt concentrations exceeded 1.0 M.

Results

A. Descriptions of the X-ray Structures. 1. [*trans*-Cr(*ms*-(5,12)-Me$_6$[14]aneN$_4$)(OH$_2$)(OH)](ClO$_4$)$_2$·H$_2$O. The atomic co-

(25) (a) Ryu, C. K.; Endicott, J. F. *Inorg. Chem.* **1988**, *27*, 2203. (b) Ryu, C. K.; Lessard, R. B.; Lynch, D.; Endicott, J. F. *J. Phys. Chem.* **1989**, *93*, 1752.
(26) Sheldrick, G. M. SHELXTL. University of Gottingen, Germany, 1978.
(27) Sheldrick, G. M. SHELX-76. University Chemical Laboratory, Cambridge, England, 1976.
(28) *International Tables for X-ray Crystallography*; Kynoch Press: Birmingham, England, 1974; Vol. IV (present distributor D. Reidel, Dordrecht).
(29) (a) Endicott, J. F.; Kumar, K.; Schwarz, C. L.; Perkovic, M. W.; Lin, W.-K. *J. Am. Chem. Soc.* **1989**, *111*, 7411. (b) Schwarz, C. L.; Endicott, J. F. *Inorg. Chem.* **1989**, *28*, 4011. (c) Perkovic, M. W. Ph.D. Dissertation, Wayne State University, 1990.
(30) Allinger, N. L.; Yuh, Y. H. Molecular Mechanics: Operating Instructions for MM2 and MMP2 Programs 1980 Force Field. Chemistry Department, Indiana University, Bloomington, IN; QCPE Program No. 395.
(31) Brubaker, G. R.; Johnson, D. W. *Coord. Chem. Rev.* **1984**, *53*, 1.
(32) Lever, A. B. P. *Inorganic Electronic Spectroscopy*, 2nd ed.; Elsevier: Amsterdam, 1984.
(33) See paragraph at end of paper regarding supplementary material.

Table II. Fractional Atomic Parameters for [*trans*-Cr(*ms*-(5,12)-Me_6[14]aneN$_4$)(OH)(OH_2)](ClO_4)$_2$·H_2O

atom	x	y	z	U(eq),[a] Å^2
Cr1	0.00000	0.00000	0.00000	0.0228 (3)
O1	0.0098 (3)	0.1184 (3)	0.1364 (2)	0.036 (1)
N1	−0.1652 (3)	0.0399 (3)	−0.0715 (2)	0.027 (1)
N2	0.1370 (3)	0.1587 (3)	−0.0595 (2)	0.027 (1)
C1	−0.1010 (4)	0.1284 (4)	−0.1460 (3)	0.031 (1)
C2	0.0484 (4)	0.2306 (3)	−0.0910 (3)	0.032 (1)
C3	0.2912 (4)	0.2463 (3)	−0.0043 (3)	0.033 (1)
C4	0.2975 (5)	0.3529 (4)	0.0898 (4)	0.043 (2)
C5	0.3768 (5)	0.3160 (5)	−0.0849 (4)	0.047 (2)
C6	0.3580 (4)	0.1535 (4)	0.0305 (3)	0.037 (2)
C7	0.3046 (4)	0.0787 (3)	0.1194 (3)	0.032 (1)
C8	0.4180 (5)	0.0375 (5)	0.1691 (4)	0.051 (2)
Cr2	0.00000	0.50000	0.50000	0.0237 (3)
O2	0.0164 (4)	0.3729 (4)	0.3801 (3)	0.038 (1)
N3	0.1772 (3)	0.4998 (3)	0.5931 (2)	0.029 (1)
N4	−0.1205 (3)	0.3313 (3)	0.5556 (2)	0.029 (1)
C9	0.1283 (4)	0.3640 (4)	0.6181 (3)	0.033 (1)
C10	−0.0211 (4)	0.3235 (4)	0.6451 (3)	0.035 (2)
C11	−0.2740 (4)	0.2994 (3)	0.5732 (3)	0.035 (1)
C12	−0.2796 (5)	0.3870 (5)	0.6764 (3)	0.044 (2)
C13	−0.3468 (5)	0.1518 (5)	0.5799 (5)	0.053 (2)
C14	−0.3555 (4)	0.3167 (4)	0.4730 (3)	0.039 (2)
C15	−0.3162 (4)	0.4561 (4)	0.4496 (3)	0.035 (1)
C16	−0.4375 (5)	0.4564 (6)	0.3703 (4)	0.055 (2)
Cl1	−0.1893 (1)	0.3507 (1)	0.10321 (8)	0.0427 (4)
O3	−0.2656 (4)	0.4146 (4)	0.1556 (3)	0.092 (2)
O4	−0.0433 (4)	0.4142 (5)	0.1344 (4)	0.160 (3)
O5	−0.2318 (6)	0.3167 (7)	−0.0002 (3)	0.196 (5)
O6	−0.2186 (7)	0.2306 (6)	0.1293 (7)	0.224 (5)
Cl2	0.2015 (1)	0.0454 (1)	0.62836 (9)	0.0533 (5)
O7	0.1148 (3)	0.0929 (3)	0.6905 (2)	0.059 (1)
O8	0.1108 (4)	−0.0677 (4)	0.5490 (3)	0.104 (2)
O9	0.2895 (5)	0.1460 (4)	0.5844 (4)	0.142 (3)
O10	0.2844 (6)	0.0022 (6)	0.6909 (4)	0.159 (4)
O11	0.1458 (4)	0.2084 (4)	0.3387 (3)	0.050 (1)

[a] $U(eq) = {}^1/_3\sum_i\sum_j U_{ij}a^*_i a^*_j \mathbf{a}_i\cdot\mathbf{a}_j$.

ordinates are given in Table II; bond lengths and angles for the cations are shown in Table III. The structure contains two independent half-cations, two independent perchlorates, and one water of hydration. The two independent Cr atoms occupy nonequivalent inversion centers in the lattice. Figure 3 illustrates the geometry and labeling of the cations. There is a strong network of hydrogen bonds creating linear chains of cations linked by the solvent water molecule. A portion of the infinite chain is shown in Figure 4. Hydrogen atoms have been added for completeness although their definitive arrangement on the axial ligands is unclear. Other weaker interactions between polar hydrogen atoms and oxygens are present in the structure but those H···O contacts are all well over 2.0 Å.

The two independent coordination spheres are structurally equivalent except for the hydrogen atoms on the axial oxygens. Charge balance requires that the axial sites in the two trans $Cr^{III}(N_4)$ cations be occupied by two OH^- and two H_2O ligands. The possibilities for assignment of these four ligands over the two coordination spheres are (i) *trans*-diqauo and *trans*-dihydroxo species and (ii) two equivalent aquo–hydroxo species. The latter interpretation requires the violation of inversion symmetry at the Cr centers but is chemically attractive because the postulation of disorder at these axial sites easily accounts for the nearly equal Cr–O bond distances. Because X-ray diffraction is such a weak analytical technique with regard to hydrogen placement, the ultimate interpretation of the present structure remains unclear.[34] The N–H protons indicate an (*RSSR*)[35] configuration and the (*R,S*)-*C*-methyl groups are equatorial. These arrangements are of the lowest energy and agree with the conformations for the

Table III. Bond Lengths (Å) and Angles (deg) for *trans*-Cr(*ms*-(5,12)-Me_6[14]aneN$_4$)(OH)(OH_2)$^{2+}$

Cr1–O1	1.973 (2)	Cr2–O2	1.973 (2)
Cr1–N1	2.071 (2)	Cr2–N3	2.068 (2)
Cr1–N2	2.091 (2)	Cr2–N4	2.084 (2)
N1–C1	1.497 (3)	N3–C9	1.490 (3)
N1′–C7	1.495 (4)	N3′–C15	1.503 (4)
N2–C2	1.487 (3)	N4–C10	1.491 (4)
N2–C3	1.513 (4)	N4–C11	1.517 (4)
C1–C2	1.512 (5)	C9–C10	1.509 (5)
C3–C4	1.519 (4)	C11–C12	1.527 (4)
C3–C5	1.532 (5)	C11–C13	1.532 (4)
C3–C6	1.535 (4)	C11–C14	1.541 (4)
C6–C7	1.538 (4)	C14–C15	1.526 (4)
C7–C8	1.522 (5)	C15–C16	1.524 (5)
Cr1–N1–C1	105.9 (2)	Cr2–N3–C9	105.7 (2)
Cr1–N1′–C7	116.5 (1)	Cr2–N3′–C15	116.9 (2)
Cr1–N2–C2	105.5 (2)	Cr2–N4–C10	106.0 (2)
Cr1–N2–C3	122.6 (1)	Cr2–N4–C11	122.4 (1)
O1–Cr1–N1	89.66 (9)	O2–Cr2–N3	90.1 (1)
O1–Cr1–N2	93.50 (9)	O2–Cr2–N4	86.3 (1)
N1–Cr1–N2	85.43 (9)	N3–Cr2–N4	85.68 (9)
N1–C1–C2	108.9 (2)	N3–C9–C10	109.4 (2)
N1′–C7–C6	108.2 (2)	N3′–C15–C14	110.1 (2)
N1′–C7–C8	111.9 (2)	N3′–C15–C16	110.7 (2)
N2–C2–C1	109.0 (2)	N4–C10–C9	109.7 (2)
N2–C3–C4	111.1 (3)	N4–C11–C12	112.3 (3)
N2–C3–C5	109.4 (2)	N4–C11–C13	109.1 (2)
N2–C3–C6	107.4 (2)	N4–C11–C14	107.1 (2)
C1′–N1′–C7	115.4 (2)	C9′–N3′–C15	114.5 (2)
C2–N2–C3	116.0 (2)	C10–N4–C11	115.9 (2)
C3–C6–C7	120.2 (3)	C11–C14–C15	120.1 (3)
C4–C3–C5	108.8 (2)	C12–C11–C13	108.5 (3)
C4–C3–C6	112.3 (2)	C12–C11–C14	112.1 (2)
C5–C3–C6	107.7(3)	C13–C11–C14	107.6 (3)
C6–C7–C8	110.6 (3)	C14–C15–C16	110.6 (3)

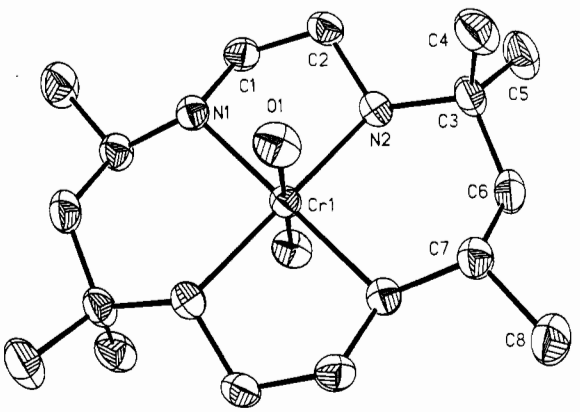

Figure 3. ORTEP diagram, with spheres at 50% probability, of one of the two independent cations in the structure of [*trans*-Cr(*ms*-(5,12)-Me_6-[14]aneN$_4$)(OH_2)(OH)](ClO_4)$_2$·H_2O. The ORTEP diagram of the second cation is included in the supplementary information. The Cr atoms each occupy inversion centers.

macrocycles in *trans*-Cr([14]aneN$_4$)($OCONH_2$)$_2^+$ [36] and Cr-(*ms*-(5,12)-Me_6[14]aneN$_4$)(OH_2)Cl^{2+}.[37]

The Cr–O lengths are identical in the two independent Cr-(*ms*-(5,12)-Me_6[14]aneN$_4$)(OH)(OH_2)]$^{2+}$ coordination spheres at 1.973 (2) Å. This length is significantly shorter than the 2.090 (6) Å observed for *trans*-Cr(Cl)(H_2O)(*ms*-(5,12)-Me_6[14]-aneN$_4$)$^{2+}$,[37] which might be exhibiting a structural trans effect. Shorter Cr–O lengths are recorded for *trans*-Cr($OCONH_2$)$_2$-([14]aneN$_4$)$^+$, Cr–O = 1.959 (2) Å,[36] *cis*-Cr(*rac*-(5,12)-Me_6-[14]aneN$_4$)(OH)$_2^+$, Cr–O = 1.918 (2) Å,[38] and *cis*-Cr(*rac*-(5,12)-Me_6[14]aneN$_4$)(O_2CO)$^+$, Cr–O = 1.952 (2) Å.[38] The structure

(34) The following reference offers an alternative interpretation of a similar hydroxo/aquo ambiguity: Ardon, M.; Bino, A. *Inorg. Chem.* **1985**, *24*, 1343.
(35) House, D. A.; McKee, V. *Inorg. Chem.* **1984**, *23*, 4237.
(36) Bang, E.; Mønsted, O. *Acta Chem. Scand.* **1982**, *A36*, 353.
(37) Temple, R.; House, D. A.; Robinson, W. T. *Acta Crystallogr.* **1984**, *C40*, 1789.
(38) Bang, E.; Mønsted, O. *Acta Chem. Scand.* **1984**, *A38*, 281.

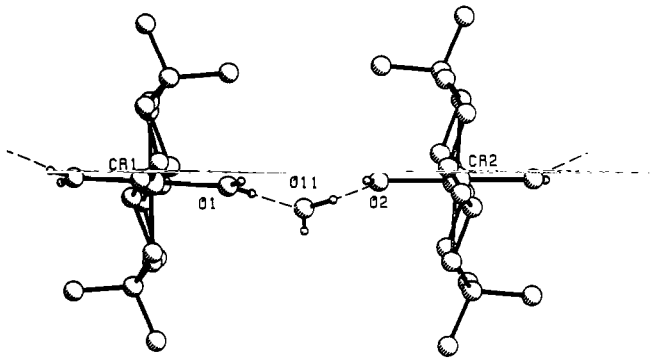

Figure 4. Portion of the linear chain of *trans*-Cr(*ms*-(5,12)-Me_6[14]-aneN_4)$(OH_2)(OH)^{2+}$ cations linked by hydrogen bonds to the water of hydration (O11). Atomic spheres are arbitrarily sized. Note that the geminal methyl groups restrict access to the axial coordination sites.

Table IV. Fractional Atomic Parameters for [*cis*-Cr(*rac*-(5,12)-Me_6[14]aneN_4)$(CN)_2$]Cl

atom	*x*	*y*	*z*	*U*(eq),[a] Å^2
Cr1	0.00000	0.00000	0.00000	0.0185 (2)
Cl1	0.00000	0.3338 (1)	0.00000	0.0444 (6)
N1	0.0626 (3)	0.1084 (2)	−0.04271 (7)	0.0195 (9)
N2	0.2143 (3)	0.0170 (2)	0.02004 (7)	0.0205 (9)
N3	0.1207 (4)	−0.1796 (3)	−0.0545 (1)	0.046 (1)
C1	0.2201 (3)	0.1078 (3)	−0.04256 (9)	0.026 (1)
C2	0.2714 (3)	0.1082 (3)	−0.0011 (1)	0.027 (1)
C3	0.2506 (4)	0.0213 (3)	0.06290 (8)	0.023 (1)
C4	0.2295 (5)	−0.0879 (4)	0.0797 (1)	0.038 (1)
C5	0.4083 (4)	0.0502 (3)	0.0681 (1)	0.030 (1)
C6	0.1599 (4)	0.1042 (3)	0.0831 (1)	0.025 (1)
C7	−0.0036 (4)	0.0927 (2)	0.08278 (8)	0.023 (1)
C8	−0.0672 (4)	0.1677 (4)	0.11132 (9)	0.038 (1)
C9	0.0730 (4)	−0.1182 (3)	−0.0359 (1)	0.026 (1)

[a] $U(eq) = {}^1/_3\sum_i\sum_j U_{ij}a^*_i a^*_j \mathbf{a}_i\cdot\mathbf{a}_j$.

of guanidinium hexaaquochromium(III) sulfate[39] contains the $Cr(H_2O)_6^{3+}$ ion and is a relatively recent $Cr(H_2O)_6^{3+}$ ion determination. Its Cr–O lengths vary 1.93–1.98 Å. Most literature Cr(III)–hydroxo bonds are present in μ-hydroxo complexes, and these show a large variability in Cr–O lengths. Normal values for Cr(III)–OH_2 and Cr(III)–OH lengths are not well-known and seem to be dependent on the other lattice components, especially those with hydrogen-bonding capabilities.

The two perchlorate anions show their typical poor refinement. There is obvious disorder in this region and subsequent high thermal parameters for the perchlorato oxygen atoms. Alternate sets of positions for these atoms were evident in the final ΔF map, but placement of partial atoms did not significantly improve the model. Average perchlorate parameters are Cl–O = 1.373 (40) Å and O–Cl–O = 109.4 (4.0)°.

2. *cis*-Cr(*rac*-(5,12)-Me_6[14]aneN_4)$(CN)_2$]Cl. Table IV contains the atomic coordinates, while Table V lists bond lengths and angles. Figure 5 shows the adopted labeling and geometry of the cation. The asymmetric unit contents consist of one independent half-cation and one half-chloride. Both Cr and Cl occupy positions on the crystallographic 2-fold axis. The CN ligands are cis, and the macrocycle is folded about the N2–Cr–N2′ line, making N1 and N1′ trans to the CN ligands. The amine protons show close contacts to the Cl^- anion, indicating probable hydrogen bonds (Cl···H1N1 = 2.385 Å, Cl···H1N2 = 2.323 Å). The configuration at the N atoms is (*SSSS*). The set of components mirror-related to these configurations is also present in the lattice. The lone methyl substituents (C8 and C8′ in Figure 5) are in equatorial positions. There is a slight tetrahedral distortion of the CrN_2C_2 coordination plane. Atoms C9 and C9′ lie ± 0.178 (4) Å out of the N1–Cr–N1′ plane. The macrocyclic

(39) Schein, B. J. B.; Lingafelter, E. C.; Stewart, J. M. *J. Chem. Phys.* **1967**, *47*, 5183.

Table V. Bond Lengths (Å) and Angles (deg) for *cis*-Cr(*rac*-(5,12)-Me_6[14]aneN_4)$(CN)_2^{2+}$

Cr1–N1	2.119 (3)	C1–C2	1.518 (5)
Cr1–N2	2.135 (2)	C3–C4	1.534 (5)
Cr1–C9	2.082 (3)	C3–C5	1.533 (5)
N1–C1	1.474 (4)	C3–C6	1.534 (5)
N2–C2	1.484 (4)	C6–C7	1.537 (5)
N2–C3	1.528 (4)	C7–C8	1.506 (5)
N3–C9	1.115 (5)	N1′–C7	1.511 (4)
Cr1–N1–C1	105.7 (2)	N2–Cr1–N2′	168.2 (1)
Cr1–N1′–C7	117.2 (2)	N2–Cr1–C9	87.8 (1)
Cr1–N2–C2	104.9 (2)	N2–Cr1–C9′	100.9 (1)
Cr1–N2–C3	122.0 (2)	N2–C2–C1	110.7 (3)
Cr1–C9–N3	175.6 (4)	N2–C3–C4	108.0 (3)
N1–Cr1–N1′	97.7 (1)	N2–C3–C5	109.8 (2)
N1–Cr1–N2	84.3 (1)	N2–C3–C7	110.4 (3)
N1–Cr1–N2′	88.0 (1)	C1′–N1′–C7	111.6 (2)
N1–Cr1–C9	88.3 (1)	C2–N2–C3	112.0 (2)
N1–Cr1–C9	172.2 (1)	C3–C6–C7	118.7 (3)
N1–C1–C2	108.7 (2)	C4–C3–C5	107.5 (3)
		C4–C3–C6	113.0 (3)
		C5–C3–C6	108.1 (3)
N1′–C7–C6	111.0 (3)	C6–C7–C8	109.1 (3)
N1′–C7–C8	112.1 (3)	C9–Cr1–C9′	86.1 (1)

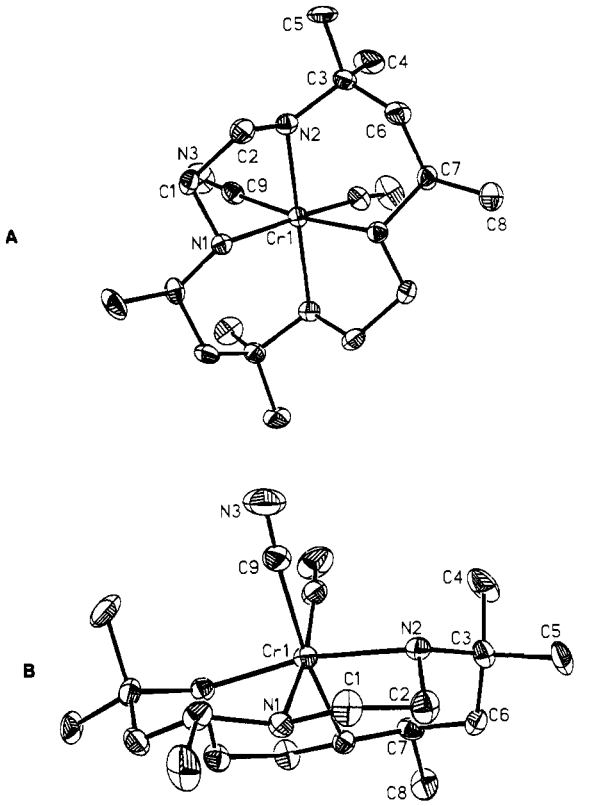

Figure 5. ORTEP drawings at 50% probability of the cation in the structure of [*cis*-Cr(*rac*-(5,12)-Me_6[14]aneN_4)$(CN)_2$]Cl. The central Cr atom occupies a crystallographic 2-fold rotation axis. Views are along the C_2 axis (A) and perpendicular to the C_2 axis (B). Note that the geminal methyl groups restrict access to the CN^- coordination sites, but the side of the molecule opposite to the cyanides appears relatively free of such stereochemical restrictions.

conformation is entirely similar to that of *cis*-$Cr(OH)_2$(*rac*-(5,12)-Me_6[14]aneN_4)$^+$ [38] and *cis*-$Cr(O_2CO)$(*rac*-(5,12)-Me_6-[14]aneN_4)$^+$.[38]

The "folding" conformation (vide infra) of the *rac*-(5,12)-Me_6-[14]aneN_4 macrocycle has been described by two parameters, α and δ.[38] δ measures the position of the metal with regard to the midpoint (represented here as M*) of the trans N–N donor atoms, and α is the fold angle calculated by the angle N_{cis}–M*–N_{cis}. For this structure, δ = Cr···M* = 0.219 (2) Å and α = N1–M*–N1′ = 107.2 (2)°. These parameters are likewise very similar to those calculaetd for *cis*-$Cr(OH)_2$(*rac*-(5,12)-Me_6[14]aneN_4)$^+$ (δ

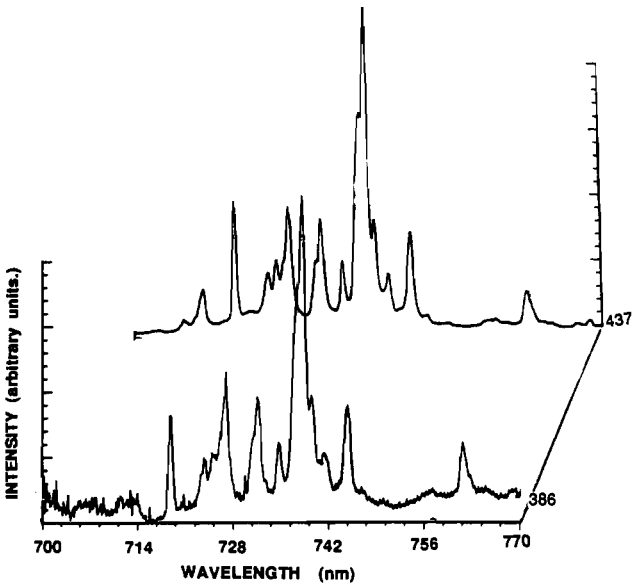

Figure 6. Emission spectra at 77 K of 3% *trans*-Cr([14]aneN$_4$)(CN)$_2^+$ doped into [*trans*-Rh([14]aneN$_4$)(CN)$_2$]PF$_6$. Intensities have been corrected for detector response. The peak at 712 nm had an excitation-wavelength-dependent intensity and is attributed to an impurity emission. Powder deuterioamine samples: 437-nm excitation (top); 386-nm excitation (bottom).

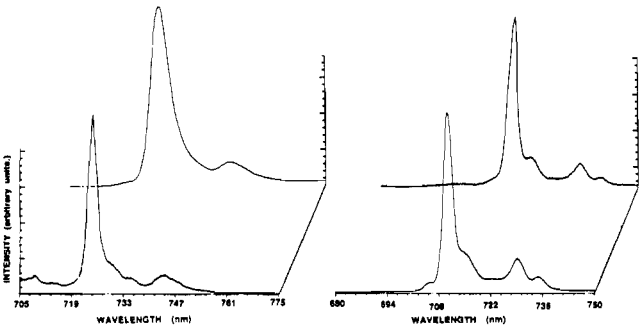

Figure 7. Emission spectra of noncentrosymmetric Cr(N$_4$)(CN)$_2^+$ complexes at 77 K. Left side, *cis*-Cr(*rac*-(5,12)-Me$_6$[14]aneN$_4$)(CN)$_2^+$: deuterioamine in DMSO/H$_2$O (1:1, v/v), upper spectrum; deuterioamine doped (3%) into [*cis*-Rh(*rac*-(5,12)-Me$_6$[14]aneN$_4$)(CN)$_2$]ClO$_4$, lower spectrum. Right side, *trans*-Cr([15]aneN$_4$)(CN)$_2^+$: solid perchlorate salt, upper spectrum; complex in DMSO/H$_2$O (1:1, v/v), lower spectrum. All excitations were at 406 nm.

= 0.274 Å and α = 106.6°) and *cis*-Cr(O$_2$CO)(*rac*-(5,12)-Me$_6$-[14]aneN$_4$)$^+$ (δ = 0.189 Å and α = 107.7°).[38]

The Cr—C bond length of 2.119 (3) Å and C≡N length of 1.115 (5) Å are typical and agree closely with those parameters for Cr(CN)$_6^{3-}$ (Cr—C = 2.078 (4) Å, C≡N ≃ 1.142 (1) Å).[40] The Cr—C≡N angle of 175.6 (4)° is somewhat nonlinear and also typical.[41]

B. Emission Spectra. Emission spectra have been determined for the Cr(III) complexes at 77 and 298 K (Figures 6–8). The emissions from solutions and solids containing *trans*-Cr([14]-aneN$_4$)(CN)$_2^+$ have presented a number of problems. This is a relatively weak emitter (at 77 K the emission yield of this complex was found to be 5% of that of a Cr([9]aneN$_3$)$_2^{3+}$ complex[4c]), and the onset of significant absorption occurs at relatively high energy for *trans*-Cr([14]aneN$_4$)(CN)$_2^+$ (lowest energy absorption maximum at 414 nm; ϵ = 62.5). As a consequence, signal to noise problems were greatest for this complex, and the resulting emission spectra were found to be especially sensitive to impurity emissions

(40) Figgis, B. N.; Kucharski, E. S.; Patrick, J. M.; White, A. H. *Aust. J. Chem.* **1984**, *37*, 265.

(41) A search of the Cambridge Crystallographic Database produced 893 M—C≡N terminal groups with MCN angles ranging from 165 to 180° and a mean angle of 176 (2)°.

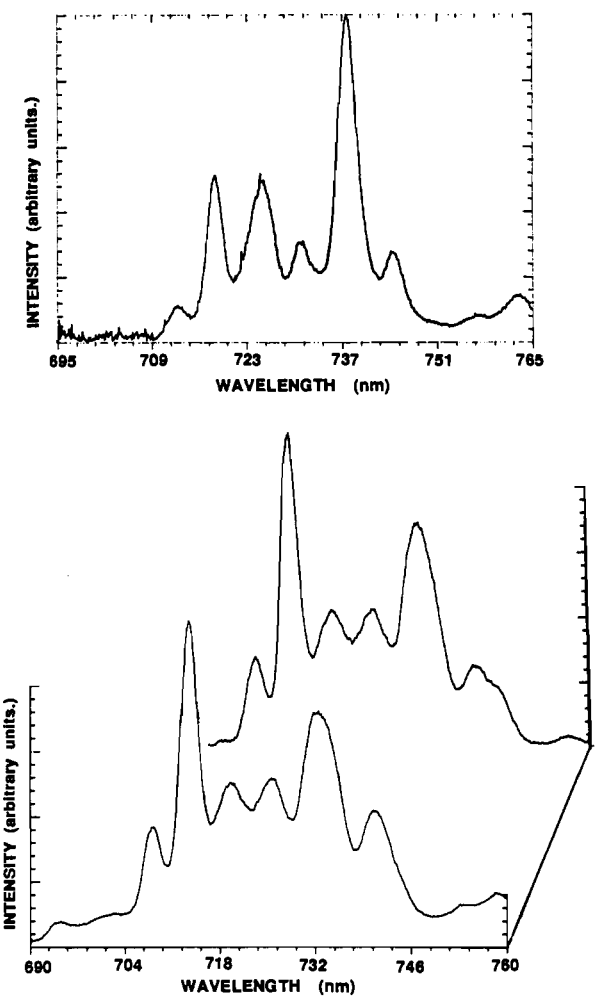

Figure 8. Emission spectra of centrosymmetric Cr(N$_4$)(CN)$_2^+$ complexes in DMSO/H$_2$O (1:1, v/v) glasses at 77 K: top, *trans*-Cr([14]aneN$_4$)-(CN)$_2^+$ (386-nm excitation); bottom, *trans*-Cr(*ms*-(5,12)-Me$_6$[14]-aneN$_4$)(CN)$_2^+$ protioamine complex (437-nm excitation; upper spectrum) and deuterioamine complex (406-nm excitation; lower spectrum).

for our usual range of excitations (437–486 nm). This may account for the relatively poor quality spectra reported previously for this complex.[4a,b,16,42] We found that careful purification and sample handling can result in good-quality spectra in which the only significant emissions are in the 680–780-nm region. Even when the emission spectrum appeared to be of good quality, with narrow well-resolved bands (resolution limit of 2.6 cm^{-1}) as in Figure 6, some of the "resolved components" turned out to be spurious. The most persistent of these bands in our samples was an emission band at 710–712 nm. The *relative* intensity of this band increased as the excitation wavelength increased ($\lambda_{ex} \geq 437$ nm), and the emission maximum was nearly identical to those of the *trans*-Cr([15]aneN$_4$)(CN)$_2^+$ emissions produced in similar situations (Figure 7). A small amount of a [15]aneN$_4$ in the samples of [14]aneN$_4$ is quite plausible,[43] and the respective dicyano complexes are similar enough in solubility and other properties that they would be difficult to separate by recrystal-

(42) Tuszynski, W.; Strauss, E. *J. Lumin.* **1988**, 276.

(43) Our sample of [14]aneN$_4$ was prepared from technical grade 1,5,8,12-tetraazaduodecane which could have easily contained a small amount of tetraazaterdecane impurity. The resulting macrocyclic complexes are very similar in properties, and small amounts of such impurities are also very difficult to remove. Related problems could in principle arise in the synthesis of *rac*- and *ms*-(5,12)-Me$_6$[14]aneN$_4$ (from condensation of acetone and ethylenediamine hydrobromide followed by NaBH$_4$ reduction), since technical grade ethylenediamine was used and since small amounts of other ligand isomers can be formed; in this instance, one expects small amounts of the 5,5,7,12,14,14-hexamethyl-1,4,8,11-tetraazacyclotetradecane ligands to result from the synthesis.[44] Configurational isomers are also a potential problem (see below).

Table VI. Selected (^{2}E)Cr(III) Emission Maxima Observed for $Cr(N_4)(CN)_2^+$ Complexes

complex	matrix	T, K	$E(^2E)$,[a] cm^{-1} (0–0′)
trans-Cr([14]aneN$_4$)(CN)$_2^+$	[*trans*-Rh([14]aneN$_4$)(CN)$_2$]PF$_6$	77	13 950 (14 022)
		298	13 974 (14 065)
	DMSO/H$_2$O (1:1, v/v)	77	13 936 (14 051)
trans-Cr(*ms*-(4,12)-Me$_6$[14]aneN$_4$)(CN)$_2^+$	DMSO/H$_2$O (1:1, v/v)	77	13 974 (14 004)
		298	13 988 (13 922)
trans-Cr([15]aneN$_4$)(CN)$_2^+$	ClO$_4^-$ salt; power	77	14 058
		298	14 066
	DMSO/H$_2$O (1:1, v/v)	77	14 039
		298	14 041
cis-Cr(*rac*-(5,12)-Me$_6$[14]aneN$_4$)(CN)$_2^+$	CF$_3$SO$_3^-$ salt; powder	77	13 862 (13 835)
	[*cis*-Rh(*rac*-(5,12)-Me$_6$[14]aneN$_4$)(CN)$_2$]PF$_6$	77	13 827
	DMSO/H$_2$O (1:1, v/v)	77	13 848

[a] Values for deuterioamine complexes in parentheses.

Table VII. Comparison of the Vibronic Origins of *trans*-Cr([14]aneN$_4$)(CN)$_2^+$ to Those of the Octahedral Parent Complexes

Cr(NH$_3$)$_6^{3+}$ [b]		Cr(CN)$_6^{3-}$ [c]		*trans*-Cr([14]aneN$_4$)(CN)$_2^+$	
$\Delta\nu$, cm^{-1}	assgnt	$\Delta\nu$, cm^{-1}	assgnt	$\Delta\nu$, cm^{-1} [a,d]	appro assgnt
		95	CCrC (t_{2u})	97 (97)	CCrC
		155	CCrC (t_{1u})		
				121 (124)	
203 (180)	NCrN (t_{2u})			175 (176)	NCrN, CCrC
261 (233)	NCrN (t_{1u})			229 (234)	CCrN, CrCN
		541	CrCN (t_{2u})	250 (249)	
		354	CrCN (t_{1u})	304 (310)	
				371 (374)	
				396 (397)	
473 (429)	CrN (t_{1u})	467	CrC (t_{1u})	432 (434)	CrC, CrN
				495 (494)	
745 (600)[d]					

[a] $\Delta\nu = E(0\text{–}0') - E$. [b] From ref 47a and the summary in ref 2. [c] From ref 47b. [d] This work; spectra from doped solids; perdeuterio vibronic origins in parentheses.

lization. As a result of these problems, we have only considered in our analysis the most prominent anti-Stokes vibronic components whose relative intensities were found to be independent of excitation wavelength. Somewhat similar problems were found for *trans*-Cr(*ms*-(5,12)-Me$_6$[14]aneN$_4$)(CN)$_2^+$.[43,44] Emission spectra of the noncentrosymmetric complexes exhibited no such problems with impurity emissions. The ^{2}E emissions of the centrosymmetric *trans*-Cr(N$_4$)(CN)$_2^+$ complexes have a great deal of intense vibronic structure and relatively weak 0–0′ lines, while complexes of lower symmetry are characterized by relatively intense 0–0′ emissions. In order to obtain the best quality spectra, we have doped several Cr(N$_4$)(CN)$_2^+$ complexes into salts of the Rh(III) analogs. Since the lowest energy Rh(III) excited states are (5–10) × 10^3 cm^{-1} higher in energy than the (^{2}E)Cr(III) excited states, the (^{2}E)Cr(III) excited states are electronically isolated when the Cr(III) is dilute (≤3%) in such salts. The emission bands tend to be broader in solution than in the solid state, but the numbers of major components in our 695–767-nm observation window were the same for *trans*-Cr([14]aneN$_4$)(CN)$_2^+$ in the crystalline and glassy matrices and the relative intensities of the major vibronic envelopes were roughly comparable.

On the basis of spectra such as those in Figures 6–8 and of comparisons of the vibronic components, we have assigned the electronic origin of (^{2}E)Cr([14]aneN$_4$)(CN)$_2^+$ as 13 950 ± 25 cm^{-1} with the slightly higher energies being found in the doped crystalline solid than in DMSO/H$_2$O and at room temperature rather than at 77 K (Table VI). This electronic origin shifts very little (≤10 cm^{-1}) upon amine deuteration. The molecular symmetry of this complex is C_{2h}, and there should be 15 coupled skeletal vibronic modes (derived from the t_{1u} and t_{2u} skeletal

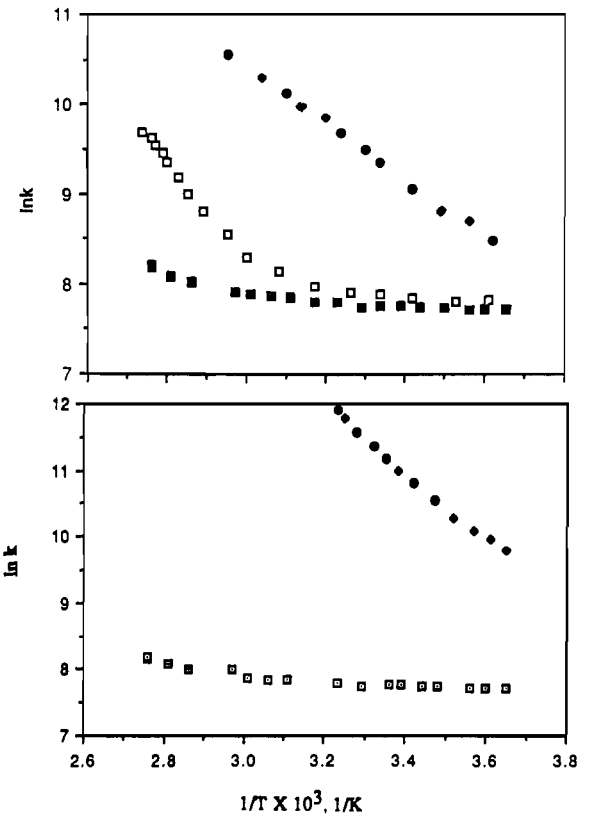

Figure 9. Variations in ^{2}E emission lifetime with acidity and temperature for Cr(Me$_6$[14]aneN$_4$)(CN)$_2^+$ complexes: top, *trans*-Cr(*ms*-(5,12)-Me$_6$[14]aneN$_4$)(CN)$_2^+$ (acid concentrations in water from top to bottom are 3.2 × 10^{-8}, 3.2 × 10^{-6}, and 2.5 × 10^{-4} M, respectively); bottom, contrasting temperature-dependent (^{2}E)Cr(N$_4$)(CN)$_2^+$ excited states for *cis*-Cr(*rac*-(5,12)-Me$_6$[14]aneN$_4$)(CN)$_2^+$ (upper curve) and *trans*-Cr(*ms*-(5,12)-Me$_6$[14]aneN$_4$)(CN)$_2^+$ (lower curve) (for both solutions, [H$^+$] = 2.5 × 10^{-4} M).

modes of O_h parentage and assuming only weak coupling with ligand modes[46]). We observed 11–13 bands in the emission spectra from doped solids which have relative intensities that are reproducibly independent of the excitation wavelength.[33] The energy differences between these bands and the band which we assign as the 0–0′ transition are consistent with expectation[46]

(44) Melson, G. A. In *Coordination Chemistry of Macrocyclic Compounds*; Melson, G. A., Ed.; Plenum: New York, 1979.

(45) We have previously determined that the radiative yields from Cr([14]aneN$_4$)(CN)$_2^+$ and Cr([15]aneN$_4$)(CN)$_2^+$ stand in a ratio of 0.21:1.[4c,25b] At 437 nm, the ratio of absorbances is about 0.5:1. Thus 90% of the emissions of an equimolar solution of these complexes would originate from Cr([15]aneN$_4$)(CN)$_2^+$. The 711-nm impurity emission in Figure 6 contributes about 3% to the total emission, suggesting that if Cr([15]aneN$_4$)(CN)$_2^+$ is the impurity, it was present at a level of about 0.3%.

(46) To the degree that low-frequency macrocyclic ligand deformations couple with the skeletal vibrations, the normal-mode assignments will be very complicated. Since the assignment of modes is not the major issue here, we have taken a relatively simple, qualitative view.

Table VIII. Photophysical Properties of Cyanoam(m)ine and Hexaam(m)ine Chromium(III) Complexes

no. in Figure 10	complex	$E(^4T_2$ or $^4A_1)_{max}$,[a] $cm^{-1}/10^3$	$E(^4T_2$ or $^4A_1)_{origin}$,[b] $cm^{-1}/10^3$	$E(^2E)$,[c] $cm^{-1}/10^3$	$\tau(298)$,[d] μs	$\tau(77)$,[e] μs	E_A,[f] kcal mol^{-1}	$k(T)$,[g] $s^{-1}/10^3$
1	$Cr(NH_3)_6^{3+}$	21.64	19.6	15.20	2.2	78	10	442
	$Cr(NH_3)_5CN^{2+}$	22.17	20.1	14.71	14		12	
	trans-$Cr(NH_3)_4(CN)_2^+$	22.5[h]	(20.2)	14.33[h]	33[h]		7[h]	
	cis-$Cr(NH_3)_4(CN)_2^+$	22.9[h]		14.29[h]				
2	*trans*-$Cr([14]aneN_4)(NH_3)_2^{3+}$	22.50[i]	20.0	14.9[i]	136[i]	180[i]		1.8
3	*cis*-$Cr([14]aneN_4)(NH_3)_2^{3+}$	21.40[i]		15.0[i]	1.0	116[i]		991
4	*trans*-Cr(*ms*-(5,12)-Me_6[14]$aneN_4)(NH_3)_2^{3+}$	22.90	19.5	14.95	31	186	7.5	27
5	*trans*-$Cr([14]aneN_4)(CN)_2^+$	24.16	21.6	13.95	361 (1724)	361 (4645)	n/a	0.36
6	*trans*-Cr(*ms*-(5,12)-Me_6[14]$aneN_4(CN)_2^+$	23.36	21.3	13.97	379 (1062)	380 (3040)	n/a	0.30
7	*trans*-$Cr([15]aneN_4)(CN)_2^+$	22.10	20.3	14.06	190	278	n/a	0.45
8	*cis*-Cr(*rac*-(5,12)-Me_6[14]$aneN_4)(CN)_2^+$	21.64	18.30	13.86	2.0	204	12	536
9	$Cr([9]aneN_3)_2^{3+}$ [j]	22.78	20.9	14.71	30.2 (30.2)	400 (3030)		33
10	$Cr([9]aneN_3CH_2-)_2^{3+}$ [k]	20.79	18.6	14.0	$[6 \times 10^{-5}]$[l]	50		$\geq 10^7$
11	$Cr(TAE[9]aneN_3)^{3+}$ [m]	21.41	18.4	14.49	$[4 \times 10^{-3}]$[l]	114		2×10^5
12	$Cr(TAP[9]aneN_3)^{3+}$ [m]	21.65	18.6	14.90	179 (850)		265 (4300)	0.94
13	$Cr(sen)^{3+}$ [n]	22.2	20.2	14.81	$[1 \times 10^{-4}]$[l]		171	$\geq 10^7$
14	$Cr(en)_3^{3+}$ [j]	21.88	19.82		1.2		120	830
15	$Cr([9]aneN_3)(CN)_3$ [o]	23.75	21.42	13.50	6.1		402	160
16	$Cr([9]aneN_3)(NH_3)_3^{3+}$ [o]	21.74	19.97	14.98	6.7		104	140

[a] Lowest energy spin-allowed absorption maximum. [b] Band origins based on energy on the red side where the absorption intensity is approximately 5% that of the absorption maximum. See refs 5, 10, and 50. [c] From Table VI, Table VII, or sources noted. [d] In H_2O or DMSO/H_2O (1:1, v/v); from this work or references as noted. Numbers in parentheses are for deuterioam(m)ine complexes in D_2O or DMSO/D_2O. [e] This work; in DMSO/H_2O (1:1, v/v) glasses except as noted. Numbers in parentheses are for deuterioam(m)ine complexes in DMDSO/D_2O glasses. [f] Approximate Arrhenius activation energy for the thermally activated (^{2}E)Cr(III) decays. Note that the onset of thermally activated decay varies from about 235 K to greater than 300 K for the compounds listed here.[4a,c,5,10] [g] $k(T) = [\tau(298)]^{-1} - [\tau(77)]^{-1}$ for protio- or deuterioam(m)ine complexes. [h] Zinato, E.; Riccieri, P.; Prelate, M. *Inorg. Chem.* **1981**, *20*, 1432. [i] Reference 7. [j] Data from refs 2–5 and: (a) Wieghardt, K.; Schmidt, W.; Hermann, W.; Küppers, H. J. *Inorg. Chem.* **1983**, *22*, 2953. (b) Ditze, A.; Wasgestian, F. *J. Phys. Chem.* **1985**, *89*, 426. [k] References 5c, 6b and: Perkovic, M. W.; Ryu, L. K.; Endicott, J. F. Work in progress. [l] Value extrapolated from temperature dependencies of τ near 200 K. [m] Reference 6a. [n] Reference 6b. [o] Ryu, C. K. Ph.D. Dissertation, Wayne State University, 1987.

based on the $Cr(NH_3)_6^{3+}$ [47a] and $Cr(CN)_6^{3-}$ [47b] parent complexes as noted in Table VII. This provides some additional support for our assignment of the band origin.

The ^{2}E emission spectra of *trans*-Cr(*ms*-(5,12)-Me_6[14]-$aneN_4)(CN)_2^+$ (Figure 8 and Table VI) were very similar in DMSO/H_2O to those of the [14]$aneN_4$ analog, as might be expected on the basis of the very similar microenvironments. The significantly stronger 0–0′ line probably reflects the somewhat lower symmetry (C_i compared to C_{2h}). The ^{2}E emission spectra of the dicyano complexes lacking a center of symmetry were dominated by a very strong 0–0′ line (Figure 9). The observed spectra are summarized in Table VIII.

Only broad vibronic envelopes were observed in DMSO/H_2O glass. Such broadening is reasonably typical. This spectroscopic broadening is not correlated with significant variation of excited-state lifetimes, even in ambient solutions where the emission is very broad for the dicyano complexes.

The 77 K lifetimes of the (^{2}E)Cr(III) complexes considered here vary between 200 and 400 μs, with the centrosymmetric complexes being the longest lived. Amine perdeuteration increased the lifetimes 8–15-fold, consistent with a tunneling mechanism for the relaxation of nearly undistorted excited states as discussed in detail elsewhere.[25b] The observed spectra are summarized in Table VIII.

C. Emission Lifetimes. The fluid-solution lifetimes of all the amine complexes were strongly pH dependent. The ^{2}E excited-state lifetimes tended to decrease as the pH increased (presumably due to deprotonation of amine functions). This was most noticeable in the relatively long-lived *trans*-(^{2}E)$(Cr(N_4)(CN)_2^+$ complexes (Figure 9 (top)). In strongly acidic solutions (pH < 3) the cyano complexes hydrolyzed, forming more weakly emitting aquo–cyano and diaquo complexes. Photophysical properties of the complexes are summarized in Table VIII. Deaeration had no detectable effect on the lifetimes at 25 °C.

The fluid-solution excited-state behavior of *cis*-(^{2}E)Cr(*rac*-(5,12)-Me_6[14]$aneN_4)(CN)_2^+$ is more similar to that of the pentaammines than to that of the trans tetraazamacrocyclic complex analogs in the sense that the decays are thermally activated in fluid solution at all pH values ≤7. An example of the contrasting behavior of these cis and trans cyano complexes is shown in Figure 9 (bottom).

D. Molecular Mechanics Calculations. We have structured the molecular mechanics calculations to examine various ways in which the macrocyclic ligands might stereochemically influence the excited-state relaxation rates in possible associative or dissociative reaction processes. The final energy for each calculation was taken to be the value obtained after the subtraction of the contributions of either the departing or the incoming ligand from the total steric energy. A FORTRAN program (DIPOLE) was written to expedite subtraction of these contributions. The results are summarized in Table IX and in the supplementary information.[33] For simplicity, the actual calculations were performed for $Cr(N_4)(Cl)_2^+$, rather than for dicyano complexes. From a stereochemical point of view, Cl^- is larger than CN^-, so one would expect slightly smaller van der Waals repulsions in the cyano complexes and this should lead to somewhat smaller amplitude differences in the residual steric energies for the cyano complexes than those we calculated for the chloro complexes.

We have also examined the tendency of the coordinated macrocyclic ligands to distort in the hypothetical 5-coordinate intermediates by removing the N–Cr–N angle constraints. There was some folding of the macrocyclic ligand in the 5-coordinate fragments for all the cis and the trans complexes. However, much larger amplitude changes in macrocyclic ligand positions were found for the *cis*-$Cr^{III}(N_4)X$ complexes. The changes in N

(47) (a) Flint, C. D.; Greenough, P. *J. Chem. Soc., Faraday Trans. 2* **1972**, *68*, 897. (b) Flint, C. F.; Greenough, P. *J. Chem. Soc., Faraday Trans. 2* **1974**, *70*, 815.

Table IX. MM2-Calculated Differences in Residual Steric Energies for $Cr^{III}(N_4)X_2^{n+}$ Complexes

complex	steric energy change,[a] kcal mol^{-1} for 5-coord (Sq-Py) intermed[b]	for Sq-Py relaxn[c]	for 7-coord intermed[d]	$\delta(\Delta G_{nr}^{\ddagger})$,[e] kcal mol^{-1}
trans-Cr([14]aneN$_4$)Cl$_2^+$	−1.16	−1.5	10.39	0[f]
trans-Cr(*ms*-(5,12)-Me$_6$[14]aneN$_4$)Cl$_2^+$	−2.46	−3.5	12.13	+0.11[f]
cis-Cr([14]aneN$_4$)Cl$_2^+$	−1.86	−1.9	5.45	
cis-Cr(*rac*-(5,12)-Me$_6$[14]aneN$_4$)Cl$_2^+$	−4.83	−5.0	5.45	−4.3[f]
trans-Cr([14]aneN$_4$)(NH$_3$)$^{3+}$	−1.10	−0.8	11.51	0
trans-Cr(*ms*-(5,12)-Me$_6$[14]aneN$_4$)(NH$_3$)$_2^{3+}$	−1.36	−1.4	12.77	−1.6
cis-Cr([14]aneN$_4$)(NH$_3$)$_2^{3+}$	−2.36	−1.2	9.73	3.7
cis-Cr(*rac*-(5,12)-Med$_6$[14]aneN$_4$)(NH$_3$)$_2^{3+}$	−6.70	−4.1	9.70	

[a] Steric energy changes, ΔE_s, computed from the difference in the residual steric energies of the final and initial structures of the reacting complex. The residual steric energies are defined as the total steric energy of the hypothetical complex (with specified bond distances, angles, etc.) less the steric interactions of the leaving group (for the 5-coordinate case) or of the entering group (for the 7-coordinate case). [b] Final state with leaving group at 3.4 Å from Cr(III) and normal N–Cr–L angle constraints; CrN_4X residue not allowed to relax. [c] Ligand steric energy differences between the square pyramidal $Cr(N_4)X$ residue and the $Cr(N_4)X$ complex which result when the N–Cr–L angle constraints are relaxed; all L–Cr–L′ interactions have been removed from these differences. [d] Initial state defined with the entering group 3.5 Å from Cr(III); final state with entering group 2.2 Å from Cr(III) (the entering group was H_2O). [e] $\delta(\Delta G_{nr}^{\ddagger}) = RT \ln (k_{nrd}^{ref}/k_{nrd})$, where k_{nrd} in the observed nonradiative relaxation rate of the perdeuterioamine complex and k_{nrd}^{ref} is for the appropriate *trans*-Cr([14]aneN$_4$)X$_2$ complex. [f] X = CN^-.

Table X. Medium Effects on $Cr^{III}(N_4)X_2$ Emission Lifetimes

medium	salt	concn, M	T, °C	lifetime, μs: *cis*-Cr(N$_4$)-(NH$_3$)$_2^{3+}$ [a]	*trans*-Cr(N$_4$)-(NH$_3$)$_2^{3+}$ [a]	*cis*-Cr(tet*b*)-(CN)$_2^+$ [b]
DMSO/H$_2$O (1:1)			11	3.1		
			30	0.7		
	NaSCN	5	11	2.5		
	NaSCN	2.5	11	2.47 ● 0.05		
	$NaCF_3SO_3$	2	11	3.2		
	$Na_2S_2O_3$	2	30	0.63 ● 0.02		
acetone			11	0.9		
	(H_2O)	0.11	11	2.5		
water			11	2.6	96	4.44
	NaNCS	2.5	11	2.3	96	2.43
	$NaCF_3SO_3$	2.5	11	2.6	93	3.57

[a] For N$_4$ = [14]aneN$_4$. [b] for tet*b* = *rac*-(5,12)-Me$_6$[14]aneN$_4$.

atom positions were rather complex in the *cis*-CrIII(N$_4$)X complexes with the cis N–Cr–N angle increasing to values of about 98° (larger for [14]aneN$_4$ than for *rac*-(5,12)-Me$_6$[14]-aneN$_4$). The trans N–Cr–N angles decreased slightly (to about 175°), and the N–Cr–X angle increased to about 110°.

E. Effects of Simple Nucleophiles on (^{2}E)Cr(III) Lifetimes in the Macrocyclic Complexes. Additions of NaSCN or $Na_2S_2O_3$ to solutions of the Cr(III) complexes did not alter the ^{2}E excited-state lifetimes except at very high concentrations (≥2 M). The cis complexes appeared to be a little more sensitive than the trans complexes to the added salts. The observations are summarized in Table X.

Discussion

This study has examined the stereochemical contributions to the photophysical behavior of several Cr(N$_4$)(CN)$_2^+$ complexes, where N$_4$ is a tetraazamacrocyclic ligand. We have demonstrated that variations in such simple stereochemical factors as ring size or bulky equatorial ligand substituents do not greatly alter ambient-solution lifetime behavior of *trans*-Cr(N$_4$)(CN)$_2^+$ complexes, whereas the cis geometry greatly facilitates quenching of the ^{2}E excited state.

The Ground-State Molecular Structures. Isomerization in Me$_6$[14]aneN$_4$ macrocycles arises in a number of ways. For 5,7,7,12,14,14-Me$_6$[14]aneN$_4$ molecules, there are two geometric isomers that differ in their arrangements of groups bonded to the asymmetric carbons (5 and 12). When carbons 5 and 12 can be related through an inversion, the tetraamine has the meso conformation; the dissymmetric diastereomer is a racemic mixture. These two isomeric ligands have been given the systematic abbreviations *ms*-(5,12)-Me$_6$[14]aneN$_4$ and *rac*-(5,12)-Me$_6$[14]-aneN$_4$ (or more trivially, tet*a* and tet*b*), respectively.[44] The metal-free meso tetraamine crystallizes with an internal center of symmetry such that all four nitrogen atoms are coplanar.[48] Conversely, the racemic isomer as a free molecule crystallizes with 2-fold rotational symmetry and the four nitrogens are non-coplanar, alternating ±0.66 Å from their mean plane.[49] As coordinated ligands, both of these molecules can bind in either a planar or a folded stereogeometry, which results in the trans or cis 6-coordinate complexes. Additional configurational assignments in coordinated complexes are the result of the chirality about each nitrogen donor center. Five combinations are possible for the stereochemical arrangements on the four nitrogen atoms and have been designated types I–V by Bosnich, Poon, and Tobe[50] for the ligand [14]aneN$_4$ but are equally applicable for *ms*-(5,12)-Me$_6$[14]aneN$_4$ and *rac*-(5,12)-Me$_6$[14]aneN$_4$. Types III and V are shown diagrammatically in Figure 2. Also shown in Figure 2 are diagrams of meso/rac and cis/trans isomerizations. Energetic factors that contribute to the differing stabilities of these combinations are (i) equatorial methyl substituents, (ii) five-membered rings in gauche conformations, (iii) six-membered rings in chair conformations, and (iv) chelate angles close to strain-free values of ≃86° for five-membered rings and ≃92° for six-membered rings. For the [14]aneN$_4$ ligand, type III configuration is favored in planar coordination and type V in folded coordination.[51] Only a narrow group of configurational/conformational combinations are observed for Cr^{III}(Me$_x$[14]aneN$_4$)

(48) Gluzinski, P.; Krajewski, J. W.; Urbanczyk-Lipkowska, Z. *Acta Crystallogr.* **1980**, *B36*, 1695.
(49) Krajewski, J. W.; Urbanczyk-Lipkowska, Z. *Cryst. Struct. Commun.* **1977**, *6*, 817.
(50) Bosnich, B.; Poon, C. K.; Tobe, M. L. *Inorg. Chem.* **1965**, *4*, 1102.
(51) An early review of these macrocycles is given by: Curtis, N. F. In *Coordination Chemistry of Macrocyclic Compounds*; Melson, G. A., Ed.; Plenum: New York, 1979; Chapter 4.

Table XI. Comparison of Structural Parameters for Cr^{III} Saturated Cyclam-like Complexes

complex	Cr–N, Å	N–Cr–N(en), deg	N–Cr–N(tn), deg	Cr–O, Å	type	ref
trans-Cr(*ms*-(5,12)-Me_6[14]aneN_4)(OH)OH_2^{2+}	2.079 (11)	85.56 (18)	94.44 (18)	1.973 (2)	III	*a*
trans-Cr(*ms*-(5,12)-Me_6[14]aneN_4)(Cl)OH_2^{2+}	2.082 (13)	86.2 (5)	93.8 (1.3)	2.090 (6)	III	37
trans-Cr(*ms*-(5,12)-Me_6[14]aneN_4)$(CN)_2^+$	2.083 (15)	85.3 (4)	94.8 (4)		III	*b*
trans-Cr([14]aneN_4)$(OCONH_2)_2^+$	2.059 (2)	85.53 (9)	94.47 (9)	1.959 (2)	III	*b*
cis-Cr([14]aneN_4)$(Cl)_2^+$	2.100 (4)	82.7 (1)	88.2 (3)		V	36
(–)-*cis*-Cr([14]aneN_4)$(Cl)_2^+$	2.080 (8)	83.0 (2)	89.5 (2)		V	*c*
cis-Cr(*rac*-(5,12)-Me_6[14]aneN_4)$(OH)_2^+$	2.141 (2)	83.3 (1)	86.7 (1)	1.918 (2)	V	35
cis-Cr(*rac*-(5,12)-Me_6[14]aneN_4)$(O_2CO)^+$	2.104 (9)	84.9 (6)	88.5 (1)	1.952 (2)	V	38
cis-Cr(*rac*-(5,12)-Me_6[14]aneN_4)$(CN)_2^+$	2.127 (4)	84.3 (1)	88.0 (1)		V	*a*

[a] This work. [b] The structure of [*trans*-Cr(*ms*-(5,12)-Me_6[14]aneN_4)$(CN)_2$]$(SO_3CF_3)\cdot 0.5H_2O$ contains a disordered anionic region. Space group: $P2_12_12_1$. Unit cell parameters: a = 6.8768 (5) Å, b = 17.440 (3) Å, c = 22.151 (5) Å, Z = 4, R = 0.078. We have deposited atomic coordinates for this structure with the Cambridge Crystallographic Data Center. The coordinates can be obtained on request from the Director, Cambridge Crystallographic Data Center, University Chemical Laboratory, Lensfield Road, Cambridge CB2 1EW, U.K. [c] Forsellini, E.; Parasassi, T.; Bombieri, G.; Tobe, M. L.; Sosa, M. E. *Acta Crystallogr.* **1986**, *C42*, 563.

(x = 0 or 6) macrocyclic complexes, and these are summarized in Table XI. In fact, for those complexes which have been structurally characterized, all Cr(*ms*-(5,12)-Me_6[14]aneN_4)X_2 complexes show planar coordination (*trans*-Cr(N_4)X_2), and all of the planar macrocycles are type III. Additionally, all Cr(*rac*-(5,12)-Me_6[14]aneN_4)X_2 complexes are folded, and all folded macrocycles are type V. The compatible nature of planar type III and folded type V has made these the most frequently observed combinations; however, complexes of other metals have shown more diversity than that observed to date for Cr(III), and the possible presence of small amounts of other stereochemical arrangements cannot be excluded. On average, for the data summarized in Table XI, the cis complexes show slightly longer Cr–N bond lengths and smaller N–Cr–N angles than the trans complexes. This implies that, for these 14-membered macrocycles, the folded conformation may be slightly more strained.

Photophysical Behavior of the Cr(N_4)$(CN)_2^+$ Complexes. The Cr(N_4)$(CN)_2^+$ complexes have some unusual spectroscopic features. Most notably, the centrosymmetric *trans*-Cr(N_4)$(CN)_2^+$ complexes exhibit the expected intense vibronic structure. The relatively intense vibronic structure is expected in a centrosymmetric complex, since the $^2E_g \rightarrow {}^4A_{2g}$ transition is Laporte forbidden and asymmetric vibrations relax the symmetry constraints. Most of the expected vibronic origins appear to be present in the emission spectra of *trans*-Cr([14]aneN_4)$(CN)_2^+$ doped into crystalline [*trans*-Rh([14]aneN_4)$(CN)_2$]PF_6.

The centrosymmetric Cr(N_4)$(CN)_2^+$ complexes are most remarkable for their nearly temperature-independent ^2E excited-state lifetimes, as Kane-Maquire and co-workers observed some time ago.[16] The *trans*-(^2E)Cr([15]aneN_4)$(CN)_2^+$ excited-state lifetime became temperature dependent (in DMSO/H_2O) at about 20 °C. The ambient-solution lifetimes of these complexes all increased to the millisecond time regime when the amine groups were perdeuterated. In contrast, *cis*-(^2E)Cr(*rac*-(5,12)-Me_6[14]aneN_4)$(CN)_2^+$ has a 2-μs lifetime in ambient solutions, exhibiting thermally activated decay behavior more typical of Cr(III) am(m)ines, and perdeuteration had little effect on its ambient lifetime. The unique photophysical behavior of the *trans*-Cr(N_4)$(CN)_2^+$ complexes, even more dramatically than that of *trans*-Cr([14]aneN_4)$(NH_3)_2^{3+}$,[7] strongly supports the contention[2,4-7] that stereochemical factors can play a major role in determining (^2E)Cr(III) excited-state lifetimes.

The incredible temperature-independent range of N–H isotope-dependent *trans*-(^2E)Cr(N_4)$(CN)_2^+$ excited-state lifetimes has some additional, important mechanistic implications. First, there does not appear to be a significant solvent-assisted Cr–CN d–d excited-state relaxation pathway analogous to the Ru–CN-mediated charge-transfer excited-state relaxation pathway found for (^{3}CT)Ru(bpy)$_2$(CN)$_2$ (a ^{3}CT quenching pathway which can be blocked by Ru–CN metalation).[52] The contrast may arise from the differences in changes in charge density near the M–CN moiety (large changes for CT compared to small changes for d–d excited-state relaxation). Finally, these observations seem to rule out a significant role for N–H to solvent hydrogen bonding[4a] as a significant (^2E)Cr(III) excited-state quenching channel.

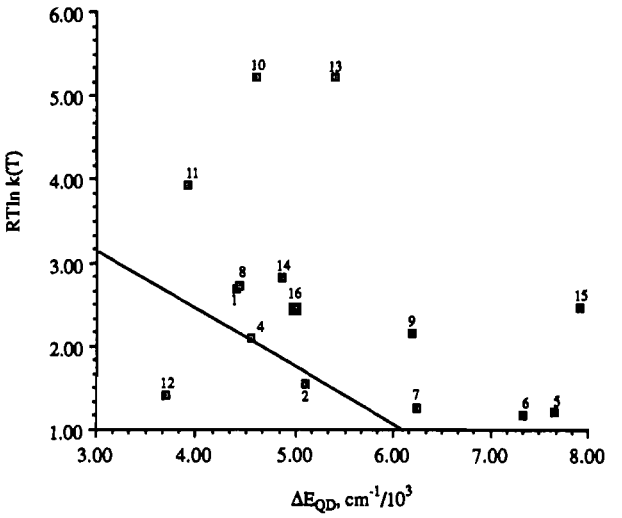

Figure 10. Comparison of the thermally activated ^2E decay rate constant, $k(T)$, to the estimated ^2E-quartet excited-state energy difference, ΔE_{QD}. Numbers refer to complexes in Table VII. The solid line is drawn on the basis of the equation $RT \ln [k(T)/A] = -\Delta E_{QD}$, where $A = 6 \times 10^{12}$ s^{-1}.

In any attempt to understand the thermally activated quenching channel (or channels), the contributions of nuclear tunneling and radiative decay should be removed; i.e., the most meaningful comparisons are of values of $k(T)$. We have determined $k(T)$ as the difference between the (^2E)Cr(III) relaxation rate constants in fluid solutions at 298 and 77 K, using data from Table VIII:

$$k(T) = [\tau(298)]^{-1} - [\tau(77)]^{-1}$$

When meaningful differences could be obtained, we found $k(T)$ to be independent of amine deuteration. For the *trans*-Cr(N_4)$(CN)_2^+$ complexes, we only obtained meaningful values of $k(T)$ for deuterioamine complexes. Values of $k(T)$ so obtained lead to some inferences about simple, limiting, relaxation pathways such as those mentioned in the Introduction. Thus, the observations on cyano–am(m)ine and hexam(m)ine complexes demonstrate that a simple BISC mechanism cannot account for the relaxation behavior of more than a small fraction of these systems, as is illustrated by the plot of the estimated excited-state quartet ($^4T_{2g}$ in O_h)–doublet state (^2E_g in O_h) energy difference, ΔE_{QD}, vs $RT \ln k(T)$ in Figure 10. The simplest BISC model (barrierless quartet excited-state decay) would predict $RT \ln [k(T)/A] = \Delta E_{QD}$ where $A \cong 6 \times 10^{12}$ s^{-1}.[53,54] This model is the basis for the solid line in Figure 10. Clearly, most of these complexes

(52) Lei, Y.; Buranda, T.; Endicott, J. F. *J. Am. Chem. Soc.* **1990**, *112*, 8820.

find a more facile relaxation pathway, and one complex, Cr(TAP[9]aneN$_3$)$^{3+}$, relaxes even more slowly than predicted by the BISC model (this implies that, at least for this complex, there is a significant barrier to quartet excited-state relaxation). It is to be noted that the approach which we have adopted for estimating ΔE_{QD}[55] results in a much smaller value than that determined in a crystalline matrix at 5 K[54] and is likely to underestimate ΔE_{QD} for most of these complexes. In fact, our previous work has shown that there is little if any influence of cis and trans stereochemistries on $k(T)$ in the Cr(N$_4$)X$_2$ complexes when ΔE_{QD} is small enough that BISC can provide the dominant relaxation channel.[12] Consequently, the present work is complementary to previous studies which have inferred that BISC is not the dominant (^{2}E)Cr(III) relaxation pathway for hexam(m)ine and cyano–am(m)ine complexes.[2,3,6,12,13]

We have also considered the possibility that relaxation might occur along some chemical reaction coordinate of the ^{2}E excited state.[56] Either an associative or a dissociative coordinate might be considered. Stereochemical perturbations introduced by the methyl substituents of the Me$_6$[14]aneN$_4$ ligands affect these reaction coordinates differently relative to the comparable reactions of the [14]aneN$_4$ complexes. The proximity of methyl groups to the axial positions in the trans complexes (see Figure 4) would lead one to expect the associative pathway to be less important in the hexamethylated than in the *trans*-Cr([14]aneN$_4$)X$_2$ complexes, and this expectation is substantiated by the MM2 calculations (Table IX). The relative values of $k(T)$ for these complexes would be most consistent with an associative reaction coordinate for X = CN$^-$ and a dissociative reaction coordinate for X = NH$_3$. The contrasts in the amplitudes of the energy differences (Me$_6$[14]aneN$_4$ complexes vs [14]aneN$_4$ complexes) calculated for "complete" reaction of the trans complexes and those observed for the effects of the methyl substituents on $k(T)$ suggests that the transition state for electronic relaxation involves only a small amount of "bond making" or "bond breaking" and that the "bond-making" (or associative) pathway is a little more important for the *trans*-Cr^{III}([14]aneN$_4$)X$_2$ complexes. Either type of reaction coordinate is predicted to be more favorable for the cis than for the trans stereochemistry. However, it must be emphasized that the energy differences considered are steric energy changes along the reaction coordinate, not the energies which result from changes in bonding. In the simplest limit, the total energy change associated with a chemical reaction which involves a change in bonding can be written

$$\Delta E_T = \Delta E_{BE} + \Delta E_s$$

where ΔE_{BE} represents the net change in chemical bond energy (including the accompanying promotion energies, changes in interelectronic repulsions, etc.) and ΔE_s is the change in steric energy. Absolute estimates of ΔE_{BE} are difficult to generate, but in the simplest limit, ΔE_{BE} is a number characteristic of the entering group for an associative pathway (or the leaving group for a dissociative pathway). A useful reference for values of ΔE_{BE} is the 26 kcal mol^{-1} activation energy (E_A) for ground-state substitution (by water) or Cr(NH$_3$)$_6^{3+}$.[57] This hydrolysis presumably proceeds through a dissociative transition state, and the associative pathway is presumed to have a slightly larger activation energy.[2] Since the ^{2}E excited state has very nearly the same metal–ligand bond lengths as the ground state[2,3,47,54,58] and since the ^{2}E excited-state potential energy surface appears to be undistorted near its minimum,[2,47,54,58] one would expect ΔE_{BE} to be similar to E_A (for the ground state) except for some relatively small corrections for interelectronic repulsion (ΔE_D, which is greater for the excited state than for the ground state). Consequently, ΔE_{BE} for NH$_3$ is probably at least 20 kcal mol^{-1} for a dissociative pathway (certainly larger than 15 kcal mol^{-1}), so that such a pathway would be energetically prohibitive for all the complexes in Table VIII, except possibly the *cis*-Cr(N$_4$)X$_2$ complexes. Given that interelectronic repulsions must increase for association with an additional ligand (about 20 kcal mol^{-1} for H$_2$O on the basis of angular overlap parameters[59]) and that these repulsions contribute to make this an ineffective pathway for ground-state substitution (so that E_A(assoc) = $\Delta E_{BE} + \Delta E_D + \Delta E_s > 26$ kcal mol^{-1}), it is difficult to see how direct reaction of the ^{2}E excited state along an associative pathway is remotely possible for any of these complexes. For example, for an associative excited-state reaction leading to electronically correlated products, one expects $E_A = \Delta E_{BE} + \Delta E_D + \Delta E_s \geq 30$ kcal mol^{-1}.

Of course, more energy than is required to activate the distortions which might lead to the substitution reactions considered above is contained in the (^{2}E)Cr(III) excited state, since its energy exceeds the activation energy required for ground-state substitution by as much as 16 kcal mol^{-1}. Crossing from the ^{2}E excited state to the region of some transition state (dissociative, associative, etc.) for a ground-state reaction amounts to a vibronically promoted spin relaxation process.[2] There are many well-established precedents for such spin relaxation processes, and their rates can vary over an enormous range, depending on the nuclear reorganizational barriers and the reactant–product energy differences.[60-62] Pertinent to the present discussion, studies from this laboratory have provided very strong evidence that a thermally activated trigonal distortion (which would form a trigonal prismatic intermediate if carried to completion) is one pathway along which the (^{2}E)Cr(III) excited state can relax.[6] No correspondingly simple correlation of structure and excited-state lifetimes is evident among the complexes considered here, but distortion toward some intermediate species with the ground-state electronic configuration seems to be the energetically most feasible type of ^{2}E relaxation pathway for these complexes. It is even plausible that both associative and dissociative ground-state reaction coordinates could be accessed from the ^{2}E excited state (along different distortion coordinates) so that the variations in response to stereochemical perturbations, which were noted above, could correspond to changes in the fractional contributions of the respective relaxation processes.

We have attempted to probe the possible roles of associative quenching pathways by examining the medium dependence of (^{2}E)Cr^{III}(N$_4$)X$_2$ lifetimes. Most of this work has focused on the *cis*-(^{2}E)Cr([14]aneN$_4$)(NH$_3$)$_2^{3+}$ complex because Waltz and coworkers reported[10] evidence for the formation of a 7-coordinate intermediate when this complex relaxed in an aqueous medium. In addition, the position of Cl$^-$ in the X-ray structure of [*cis*-Cr(*rac*-(5,12)-Me$_6$[14]aneN$_4$)(CN)$_2$]Cl, along the C_2 axis and opposite to the cyanides, seemed to suggest the possibility of facile "back-side" attack in the cis complexes.[63] We found small, but real, quenching effects of potentially nucleophilic anions (NCS$^-$

(53) This is a simple transition-state-theory argument with $A = k_B T/h$. More generally, one expects A to be an effective frequency for correlated nuclear motions (predominately an e_g vibration in O_h symmetry[54]) so that A could be plausibly placed between 5×10^{12} and 2×10^{13} s^{-1} in these complexes. See also footnote 15.
(54) Wilson, R. B.; Solomon, E. I. *Inorg. Chem.* **1978**, *17*, 1729.
(55) Fleischauer, P. D.; Adamson, A. W.; Sartori, G. *Prog. Inorg. Chem.* **1972**, *17*, 1.
(56) Gutierrez, A. R.; Adamson, A. W. *J. Phys. Chem.* **1978**, *82*, 902.
(57) Garner, C. S.; House, D. A. *Transition Met. Chem. (N.Y.)* **1970**, *6*, 59.
(58) Schmidtke, H.-H.; Adamsky, H.; Schönherr, T. *Bull. Chem. Soc. Jpn.* **1988**, *61*, 59.
(59) Vanquickenborne, L. G.; Ceulemans, A. *Coord. Chem. Rev.* **1983**, *100*, 157.
(60) Beattie, J. K. *Adv. Inorg. Chem.* **1988**, *32*, 1.
(61) Dose, B. V.; Hoselton, M. A.; Sutin, N.; Tweedle, M. F.; Wilson, L. J. *J. Am. Chem. Soc.* **1978**, *100*, 1141.
(62) Buhks, E.; Navon, G.; Bixon, M.; Jortner, J. *J. Am. Chem. Soc.* **1980**, *102*, 2918.

and $S_2O_3^{2-}$), larger for the *cis*- than for the *trans*-$Cr^{III}(N_4)X_2$ complexes; however, additions of KNCS of up to 2 M did not have discernible effect on the d–d spectra of *cis*-Cr(*rac*-(5,12)-Me_6[14]aneN$_4$)$(CN)_2^+$. Changes of the solvent appeared to have at least as large an effect on spectra[63] and the excited-state lifetimes as added anionic nucleophiles: small amounts of water actually increased the lifetime of the *cis*-(^{2}E)Cr([14]aneN$_4$)$(NH_3)_2^{3+}$ complex in acetone.[64] Nevertheless, the evidence for significant nucleophilic quenching has to be considered to be very weak. However, the observations do not preclude an associative component of the relaxation coordinate. Association with the solvent could follow (or possibly accompany) a thermally induced nuclear rearrangement. Thus, a nucleophile might intercept an intermediate formed by some thermally promoted distortions of the Cr(III) coordination sphere. If this were the case, a consequence of the expected very short intermediate lifetimes would be small nucleophilic discrimination factors and a disproportionate preference for substitution by the solvent.

Conclusions

This study very strongly supports the view that stereochemical factors contribute significantly to the ^{2}E excited-state decay patterns of macrocyclic (N_4) ligand $Cr^{III}(N_4)X_2$ complexes when X = NH_3 or CN^-. Thus, the stereochemical perturbations introduced by *C*-CH_3 groups in the aliphatic amine (N_4) ligand do alter excited-state lifetimes. In principle, these stereochemical perturbations can enhance dissociative and inhibit associative relaxation pathways, manifested here in the different relative ^{2}E excited-state lifetimes of *trans*-$Cr^{III}(N_4)X_2$ complexes in which X = NH_3 and CN^-, respectively. The greater importance of thermally activated excited-state quenching pathways to the *cis*-$Cr^{III}(N_4)X_2$ complexes than to their trans analogs (X = CN or NH_3) is also clearly a stereochemical effect; at our level of analysis, this "macrocyclic ligand" effect could be compatible with either a dissociative or an associative distortion coordinate, or with motions of the coordinated atoms along a distortion coordinate which reduces the electronic constraints for $^2E \rightarrow {}^4A_2$ relaxation. Overall, the latter possibility seems most appealing in these systems, since at least the Laporte constraint is more easily relaxed in the cis than in the trans complexes (owing to symmetry restrictions on d- and p-orbital mixing) and since (a) simple doublet-state-reaction or BISC mechanisms are difficult to reconcile with all the observations, (b) there is strong evidence that analogous distortions (i.e., $O_h \rightarrow D_{3h}$) play a dominant role in the relaxation of trigonally strained complexes, and (c) such a mechanism provides a natural explanation for the orders of magnitude contrast in the Arrhenius pre-exponential factors of the cis and trans complexes.

It is important to observe that while the observed stereochemical influences on (^{2}E)Cr(III) lifetimes clearly implicate large-amplitude nuclear displacements in the thermally activated relaxation pathway(s), they do not require that bonds be broken or formed. The observation of stereochemical influences on the excited-state lifetimes of these complexes is particularly important since back intersystem crossing ($^2E_g \rightarrow {}^4T_{2g}$ in O_h symmetry) is energetically prohibitive (or in some cases almost possible) and would have to be combined with an appreciable activation barrier for nuclear displacements to be manifested as significant stereochemical effects on the excited-state lifetimes. In fact, the varitions in observed lifetimes are consistent with expectations based on ligand stereochemistry alone.

We conclude that the most plausible thermally activated excited-state relaxation pathways in these macrocyclic cyano and ammine complexes involve nuclear distortions which promote spin relaxation and thus generate distorted species with the ground-state electronic configuration. Such relaxation coordinates are susceptible to stereochemical perturbations, and responses to stereochemical perturbations probably provide one of the best means of investigating the relaxation mechanism.

Acknowledgment. The diffractometer used herein was purchased by an NSF equipment grant to Wayne State University. The Cambridge Structural Database assisted in the literature searches. Financial support for Y.R. from the Ministry of Education of the PRC is gratefully acknowledged, and Y.R. is grateful to Lanzhou University for a leave of absence.

Supplementary Material Available: Tables A and B (thermal parameters and hydrogen parameters for [*trans*-Cr(*ms*-(5,12)-Me_6[14]aneN$_4$)$(OH)(OH_2)](ClO_4)_2 \cdot H_2O$), Tables D and E (thermal parameters and hydrogen parameters for [*cis*-Cr(*rac*-(5,12)-Me_6[14]aneN$_4$)$(CN)_2$]Cl), Table G (typical MM2 parameters), Table H (vibronic components of the ^{2}E emissions of several macrocyclic chromium(III) complexes), Table I (experimental crystallographic data for $Cr^{III}Me_6$[14]aneN$_4$ complexes), Figure A (variations in calculated residual steric energies as one Cr–X distance is increased), Figure B (variations in calculated residual steric energies as water is moved toward the Cr(III) center), and Figure C (an ORTEP diagram of the second independent cation in the structure of [*trans*-Cr(*ms*-(5,12)-Me_6[14]aneN$_4$)$(OH_2)(OH)](ClO_4)_2 \cdot H_2O$) (7 pages); Tables C and F (observed and calculated structure factors for [*trans*-Cr(*ms*-(5,12)-Me_6[14]aneN$_4$)$(OH)(OH_2)](ClO_4)_2 \cdot H_2O$ and [*cis*-Cr(*rac*-(5,12)-Me_6[14]aneN$_4$)$(CN)_2$]Cl) (25 pages). Ordering information is given on any current masthead page.

(63) There are significant solvational effects on the lowest energy quartet-state spectra of the *cis*-Cr(*rac*-(5,12)-Me_6[14]aneN$_4$)$(CN)_2^+$ complex (see the Experimental Section). However, the effects are small (they could translate into a maximum of about 1 kcal mol^{-1} change in the relative energies of the ground-state and the first quartet-state potential energy surfaces) and there is no obvious correlation of these effects with nucleophilic parameters. The only apparent correlation is that the behavior in hydrogen-bonding solvents is different from the behavior in non-hydrogen-bonding solvents.

(64) This latter result could be a consequence of ionic aggregation (e.g., a significant contribution of self-quenching) in the acetone medium, and the insensitivity of (^{2}E)$Cr^{III}(N_4)X_2$ lifetimes to the nucleophilicity of counterions could be a consequence of small discrimination factors and the large solvent concentrations; i.e., it is possible that $k_q(NCS^-) \sim 2.5k_q(H_2O)$.